

Shinnosuke Yagi
Professor Rosemary Knight
GEOPHYS 190
17 April, 2023

Assessment of Recharge Potential in the Kings Subbasin, Central Valley California

Executive Summary

Kings Subbasin, which lies in Central Valley, California, relies 75% of its water on groundwater, and 89% is used for agriculture. Their primary crops are almonds and grapes, perennial crops that consume a lot of water to produce, and this is causing severe overdraft and land subsidence across the subbasin, especially the western regions. Groundwater recharge is one effective way to address these issues in Kings Subbasin, with at least 8,000,000,000 m³ of available storage space estimated in the unconfined aquifer. To assess the potential of recharge in Kings Subbasin, we used the resistivity data collected by the airborne electromagnetic (AEM) method to construct a model of subsurface geology in the subbasin. By matching pre-existing driller's logs with resistivity data within a collocation radius of 200m, we made a histogram of resistivity of fine-dominated and coarse-dominated materials, respectively, through bootstrapping. Then we built a transform between resistivity and fraction coarse-dominated by using the median resistivity of fine-dominated and coarse-dominated materials as a tentative resistivity of each material. Through interpolation and this transform, we altered the 1-D resistivity model gained by the AEM survey into a 3-D fraction coarse-dominated model. We used three metrics (integrated fraction coarse-dominated, normalized path length, depth to no-flow) on this model to narrow down the areas suited for groundwater recharge. We also referred to SAGBI (Soil Agricultural Groundwater Banking Index) as an additional metric for evaluation. Considering the three metrics, SAGBI, proximity to the problematic western region of the basin, recharge-suited land use, and the feasibility of water conveyance, we concluded that the black circled area in the map below (ES-1) as the recommendable location for groundwater subbasin in Kings Subbasin.

Introduction

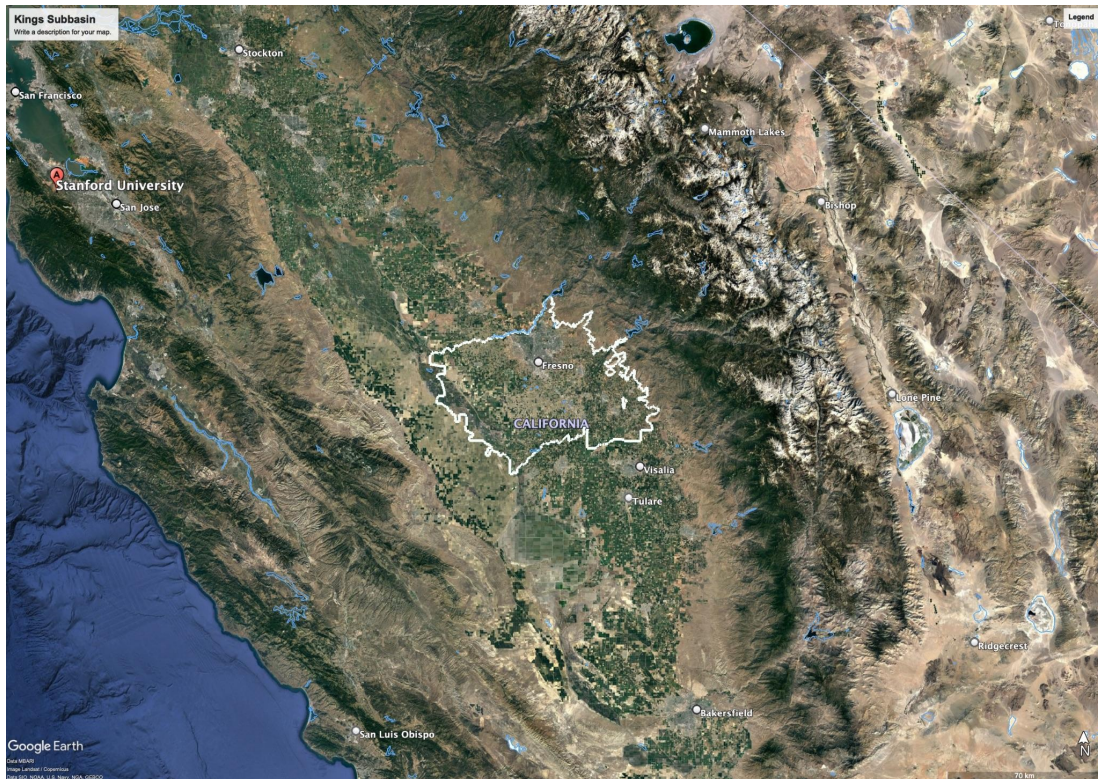
This report aims to assess the groundwater recharge potential in the Kings Subbasin and provide information on which recharged project can be planned, as well as recommendations of particular areas suited for recharge. Chapters 1 and 2 analyze the current situation of Kings Subbasin from various perspectives, including geology, geography, and economics. Chapters 3 and 4 introduce the AEM method and its usefulness in dissecting the subsurface of the Kings Subbasin. Chapters 5 to 7 explain the generation process of a 3-D fraction coarse-dominated model from AEM data in detail. Chapters 8 to 10

introduce metrics useful to evaluate recharge potential. Finally, Chapter 11 combines available metrics and factors to make a recommendation for a potential recharge site in Kings Subbasin.

1. Introducing the Subbasin

Introduction & Geography

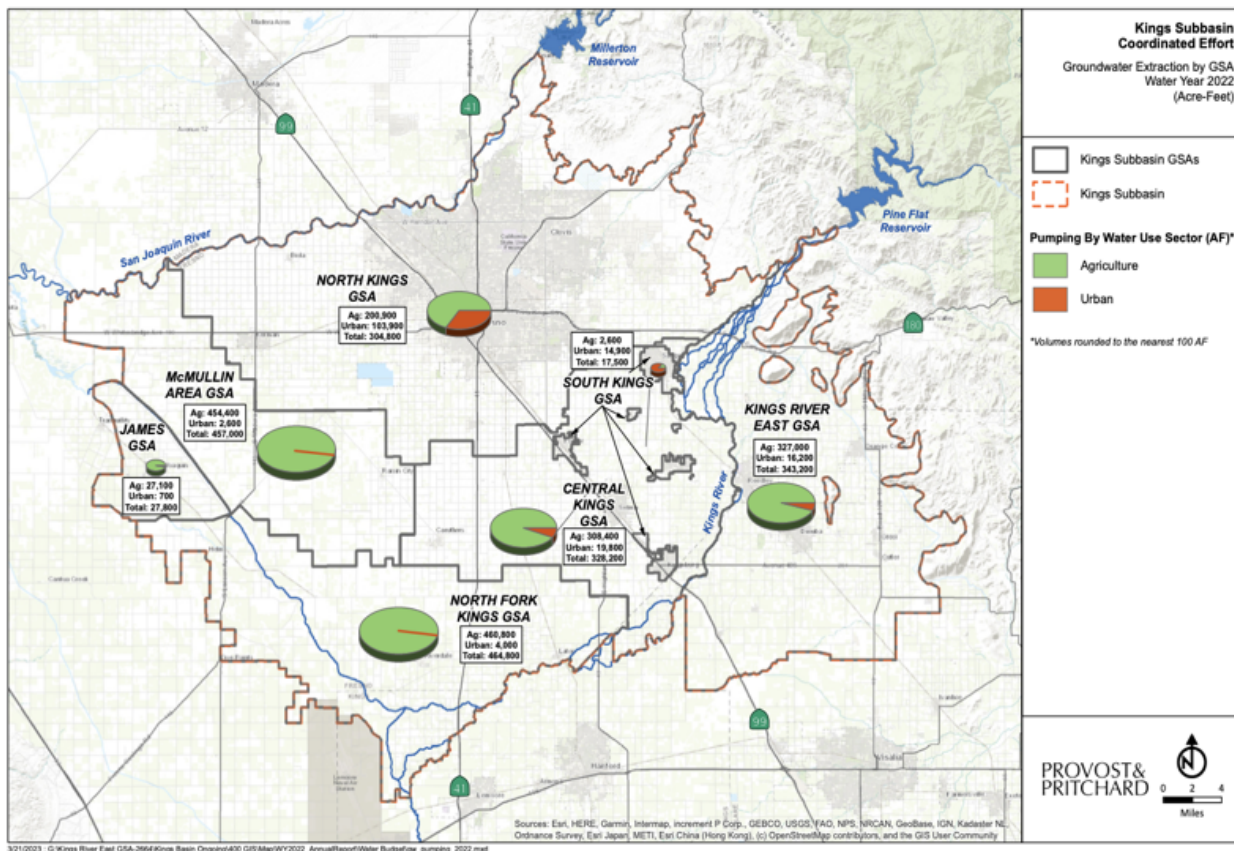
Kings Subbasin, which is a part of San Joaquin Valley, California, stretches among three counties (Fresno, Tulare, and Kings), although most of the basin belongs to Fresno County. The San Joaquin and Kings Rivers are the two principal rivers within or bordering the subbasin. The Fresno Slough and James Bypass are along the western edge of the subbasin and connect the Kings River with the San Joaquin River ([California's Groundwater Bulletin](#)). The total surface area of the subbasin is 3963 km².



(1-1, Kings Subbasin)

Kings Subbasin consists of 7 Groundwater Sustainability Agencies (GSAs): Central Kings, North Fork Kings, South Kings, McMullin Area, Kings River East, North Kings, and James ID. Each GSA has its own Groundwater Sustainability Plans (GSPs). After the incomplete determination of all seven GSPs in January 2022, GSAs took action to address the previously identified deficiencies that precluded initial approval of the Plan. As a result, all 7 GSPs received a recommendation of approval in March 2023, waiting for the final assessment to be posted (DWR). Considering that some subbasins share one GSP among the GSAs, the Kings subbasin has relatively low cooperation among the subbasin. According to the 2022 Kings Subbasin Annual Report, Total water use in the subbasin is 3,175,000,000 m³, out of

which 75% (2,397,000,000 m³) is groundwater, and 89% (2,838,000,000 m³) is agricultural use. Below is the distribution of groundwater extraction among GSAs last year.



(1-2, Kings Subbasin Groundwater Sustainability Agencies, 014)

Economy

Fresno County, which contains the majority of Kings subbasin, is the top agricultural-producing county in the United States, with \$7.98 billion in agricultural output (Fresno County Economic Development Corporation). The primary crops are almonds, cotton, grapes, cattle, plums, milk, tomatoes, turkeys, and peaches. Almonds and grapes are the top two crops on acres, and this expansion of perennial crops is one of the major causes of overdraft (United States Department of Agriculture). Fresno's unemployment rate is higher than the state average (Employment Development Department) and fluctuates on a seasonal basis due to the varying employment needs of the agricultural industry.

Disadvantaged Communities

In 2015, Fresno LAFCO identified a total of 20 DUCs (Disadvantaged Unincorporated Communities) that are located within or adjacent to the City of Fresno SOI (Sphere of Influence) and which meet the full definition of a DUC. DUCs are defined as settled places, not within city limits, where the median household income is 80 percent or less than the statewide median household income. Adequate water infrastructure is not completed in at least 14 out of 20 DUCs, implying their reliance on domestic wells (Development and Resource Management Department, City of Fresno).

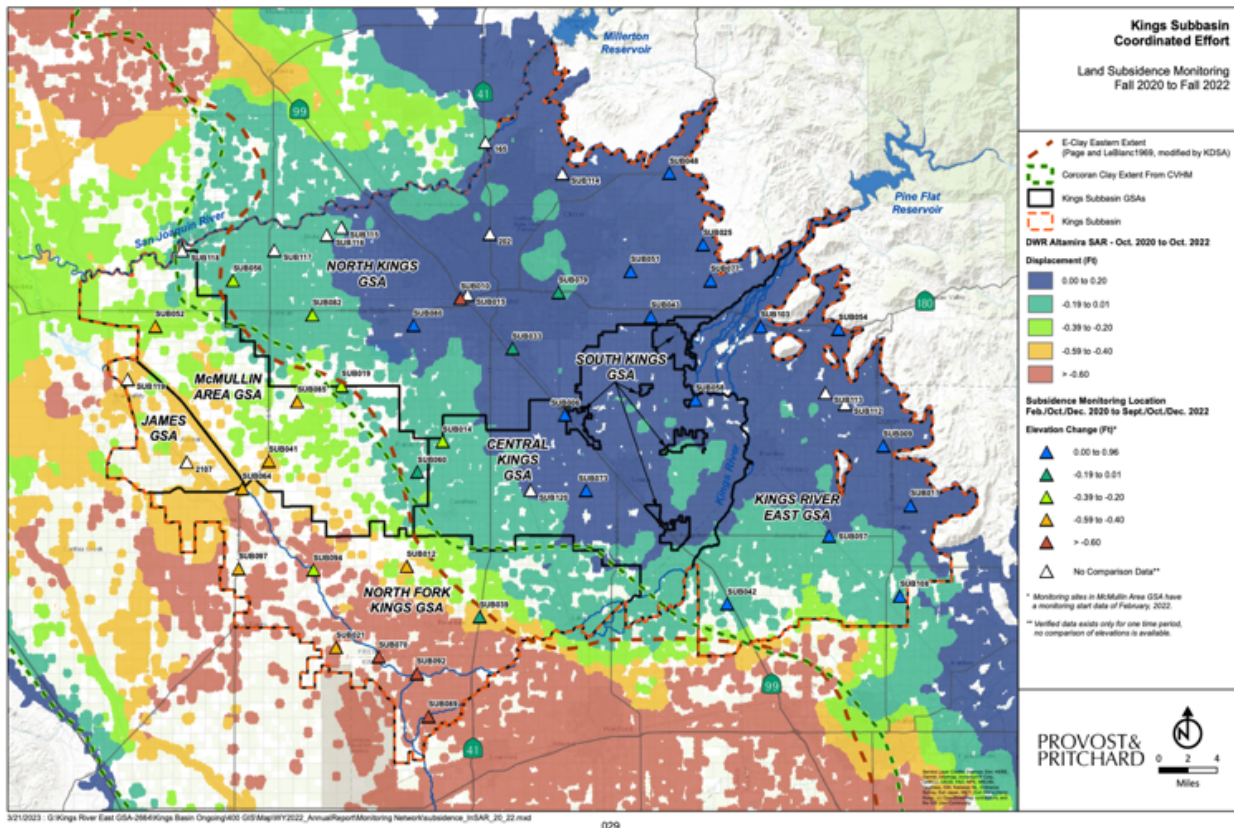
Groundwater

The largest quantity of groundwater system outflows in the Kings Subbasin is groundwater pumping. Groundwater pumping for irrigation is not directly measured for the most part and was estimated based on consumptive crop use, crop acreages, and irrigation efficiencies, with adjustments for cropland surface water deliveries. At the same time, lesser amounts of groundwater inflows (from precipitation, subsurface inflow, river seepage, and minor streams) are estimated. Below is the distribution of overdraft responsibility among GSAs provided by North Kings GSA.

GSA	Proposed Initial Responsibility (m ³)
Central Kings and South Kings	-8700000
James ID	20600000
Kings River East	-13600000
McMullin Area	-112000000
North Fork Kings	-62000000
North Kings	25700000
Total	-150000000

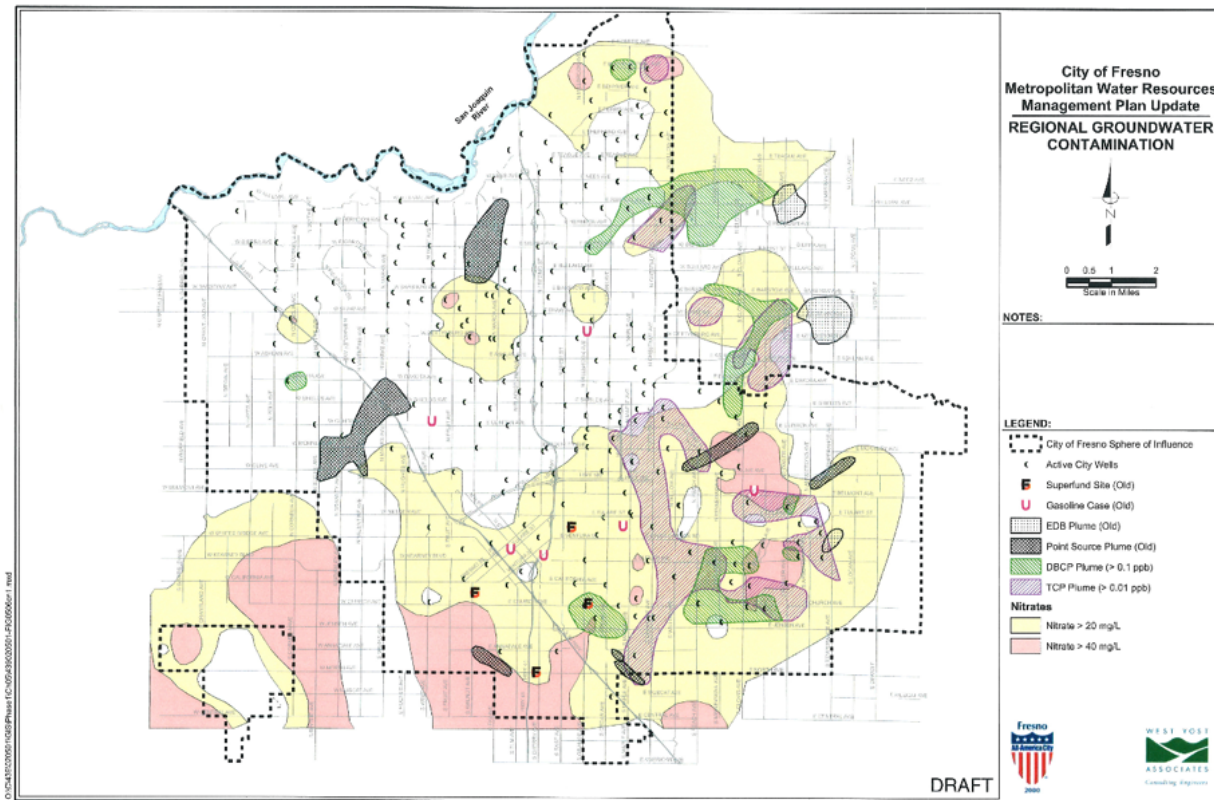
(1-3, North Kings GSA, 212)

Overdraft is leading to land subsidence in Kings subbasin, especially in the southwest area such as North Fork Kings GSA and McMullin Area GSA, as the map below shows. Land subsidence is assumed to be largely attributed to pumping outside of the Kings Subbasin, although the GSPs do not clarify the specific location of pumping.



(1-4, Kings Subbasin Groundwater Sustainability Agencies, 029)

Since Kings subbasin is one of the most urban regions in the San Joaquin Valley, groundwater contamination caused by industry and traffic might be a bigger concern. Some main constituents of contaminant plumes include nitrate, DBCP, TCP, and gasoline. These plumes either require remediation, require wellhead treatment, or limit which areas can be pumped or recharged so the plumes do not migrate.



(North Kings Groundwater Sustainability Agency, 057)

Sustainability Goal

In spite of the lack of collaboration among GSAs, they share the same sustainability goal. Below is an excerpt from the Kings Subbasin Coordination Agreement submitted by the Kings Subbasin GSAs.

The sustainability goal of the Kings Basin and each GSA is to ensure that by 2040 the basin is being managed to maintain a reliable water supply for current and future beneficial uses without experiencing undesirable results. This goal will be met by balancing water demand with available water supply to stabilize declining groundwater levels without significantly and unreasonably impacting water quality, land subsidence, or interconnected surface water. The goal of the basin is to correct and end the long-term trend of a declining water table understanding that water levels will fluctuate based on the season, hydrologic cycle, and changing groundwater demands within the basin and its proximity.

2. Initial Review of Recharge Potential in the Kings Subbasin

Geology, groundwater systems

As for surface-level soils, coarser-grained soils are found along the eastern portions of the subbasin and adjacent to the San Joaquin River and Kings River, as well as areas associated with recent alluvial deposition along intermittent streams. On the other hand, finer-grained soils are typically found in the area of the compound fan created by intermittent streams in the east and are also found in the western areas of the subbasin near the Fresno Slough (North Kings GSA, 095). From the cross-sections report in the GSP, we can learn that there are various layers of sediments and deposits from the quaternary period, such as Qoao, Qsd, and Qya, although it is hard to gain recent, precise details from here (*ibid*, 097). Three clay layers (A-clay, C-clay, and E-clay) are salient in multiple of the cross-sections taken. E-clay, or Corcoran clay, exists at a depth of approximately 150 meters near the northwestern-most portion of the North Kings GSA area, and E-clay is known to have confined groundwater conditions beneath it (*ibid*, 104).

Since Kings subbasin is relatively large compared to other subbasins, it is difficult to make a general assumption of how much available storage space is there in the unconfined aquifer for recharge over the entire basin. Therefore, we will calculate the storage space of each GSA (since their surface area is available). First, we will sample 5 co-located wells evenly from each GSA. Co-located wells are wells with a driller's log within the co-location radius from EM locations offered by DWR (further explanation in Chapter 5). *Groundwater Recharge* application by Stanford University offers the depth of the water table and fine-grained layers for these co-located wells. By choosing the smaller value of the depth of the water table or fine-grained layers for each co-located well and taking the average of 5 sampled co-located wells, we can estimate the average depth of the unconfined aquifer from the surface in the GSA. Next, we multiply it by the surface area to acquire the volume of the aquifer. Finally, we multiply this volume with a specific yield to derive the actual capacity of the unconfined aquifer. We chose 0.113 as the specific yield for Kings Subbasin, as this was the value used for the most recent modeling of the subbasin (*ibid*, 110). We omitted the South Kings GSA since its surface area is negligible (38.99146 km²), 72% of its land is urban/residential and not suited for groundwater recharge, and EM data was unavailable for most of the GSA area (South Kings GSA, 050).

The result is as below. More details are in this [spreadsheet](#). The area of each subbasin was cited from each GSA's GSP. It is important to note that this estimation is relatively conservative since we only took into account areas with permeable layers on the surface (we did not include space if a fine-dominated layer is on top, although it might be reachable).

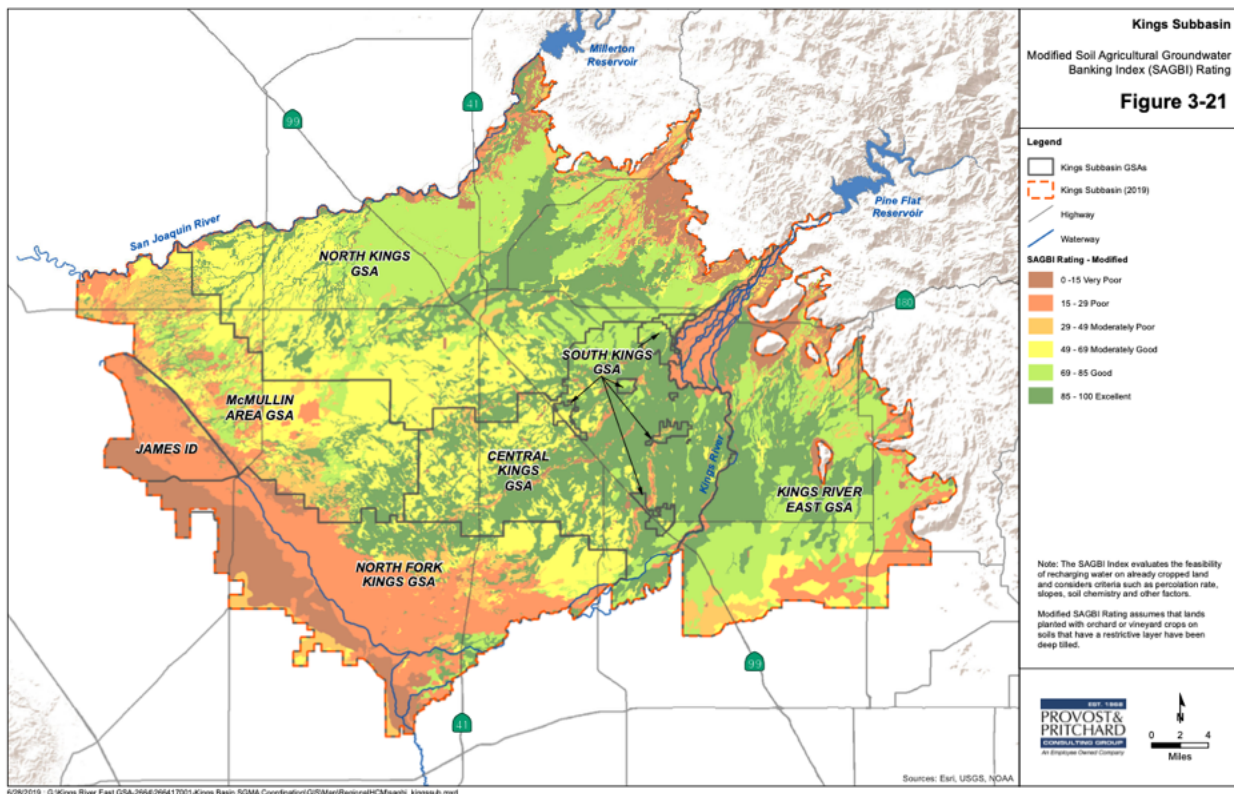
GSA	Estimated Available Storage Space (km ³)
Central Kings	0.63
James ID	0.02
Kings River East	0.30
McMullin Area	0.64
North Fork Kings	0.31

North Kings	1.70
Total	3.60

(2-1, Estimated Available Storage Space)

SAGBI

SAGBI (Soil Agricultural Groundwater Banking Index) is a composite evaluation of the feasibility of groundwater recharge on agricultural land. According to the SAGBI rating provided in North Kings GSP, a large portion of the north and east of Kings Subbasin is categorized as "good" or "excellent" for recharge, while western and southern Kings subbasin (especially James ID GSA and North Fork Kings GSA) are not suited for recharge. SAGBI is recommended to be applied in conjunction with other indexes, as it does not incorporate factors like proximity to a water conveyance system (122). In addition, some of the well-classified areas are urbanized, and recharge is not realistic.



(2-2, North Kings GSP, 124)

Recharge Efforts in Action

The Kings subbasin received a \$7.6 million dollar grant from the California Department of Water Resources (DWR) for groundwater recharge project construction on June 2022 (Quist). From the span of January 2020 (the submission of 7 GSPs) to November 2021, the Kings Subbasin Groundwater Sustainability Agencies have invested in **2.4 km²** of prime groundwater recharge land. This land represents 15 dedicated basins that are constructed or in development. Diverse funding and collaboration efforts have been made for the success of recharge projects. For example, in the Laton North Recharge

Project in the North Fork Kings GSA, builders made an agreement with a high-speed rail contractor to prepay for the dirt that will be dug through the project, which will be used to construct a section of the high-speed rail project (Kings River Conservation Project).

3. Assessing the Value of Airborne Electromagnetic Data

The Possibility and Limitations of the AEM Method

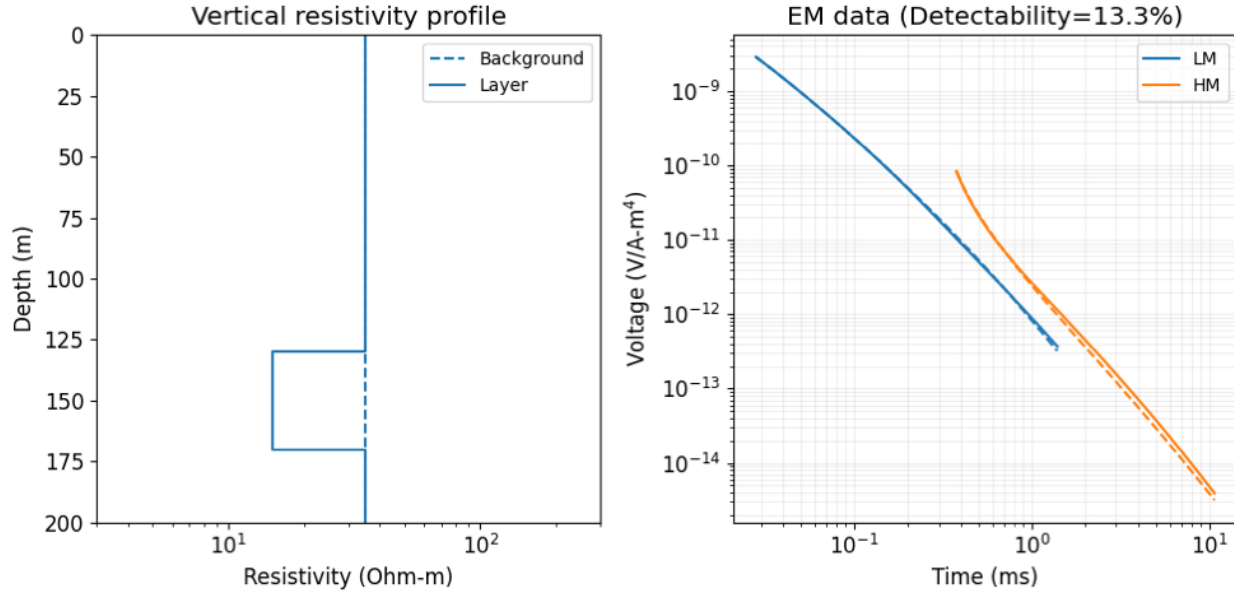
The Airborne electromagnetic (AEM) method is a type of geophysical survey used to investigate and model large-scale subsurface geology. A helicopter tows a transmitter and a receiver. A current is sent around the transmitter loop, which produces a magnetic field. This magnetic field leads to eddy currents forming in the subsurface, which then leads to secondary magnetic fields. The receiver reads a decaying voltage with time based on the decaying magnetic fields. The rate of diffusion of the secondary electromagnetic field depends on the resistivity of the subsurface composition below. Different sediments/rocks have different resistivity, and this enables us to assume the geological structure. Compared to traditional well-drilling methods, AEM data allows for more spatial continuity than well data.

Compared to the Towed EM, which uses land vehicles to pull the transmitter, the AEM method is more suited for surveys of large areas with complex terrain and geological structures. The AEM method also has a larger depth of investigation (DOI), which is the maximum depth at which AEM provides useful, reliable information about subsurface geology. One simple equation to acquire DOI is $z = \sqrt{2t/\mu\gamma}$, although various factors such as the actual geometry, noises, and the number of data points are not considered (Auken, Christiansen). DOI is crucial to process the data and grasp its reliability accurately. Drilling a well with an expectation of a rechargeable aquifer 200m deep when the DOI is 150m is irrational. The precision of the device can also limit the AEM method. Some sediment type differences do not entail salient resistivity contrast that the AEM method can detect. This limitation is also crucial for the appropriate application of the AEM method. We need to recognize the possibility that a seemingly rechargeable aquifer is actually not accessible due to a hidden clay layer that the AEM method did not capture.

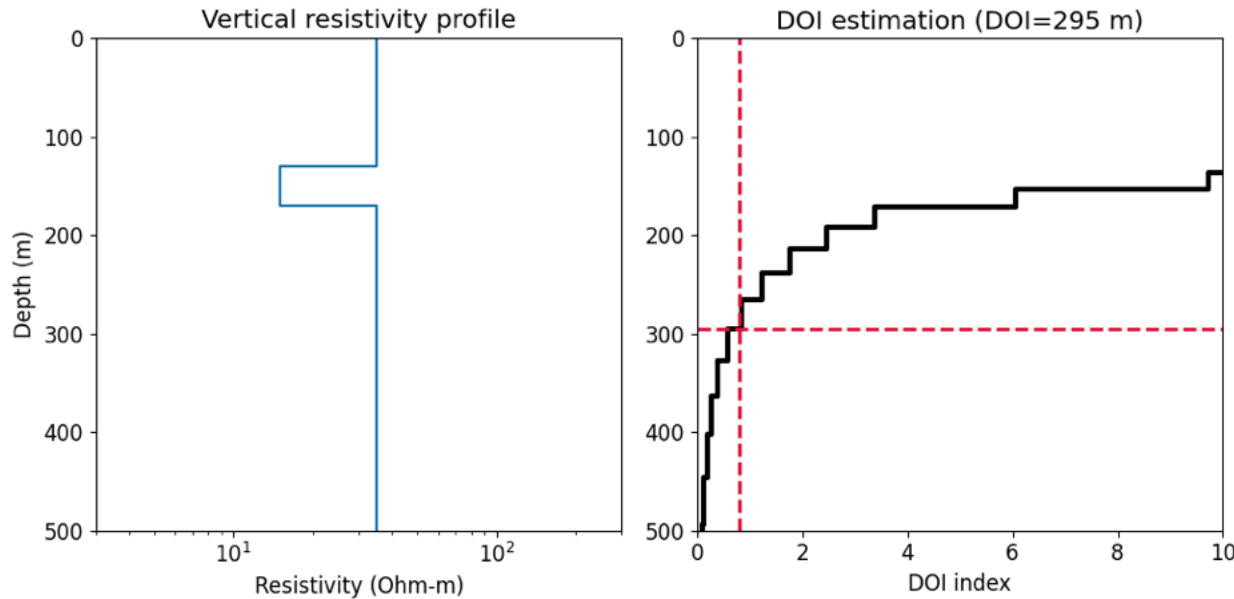
Application of AEM Method in Kings Subbasin

As we plan a groundwater recharge in the Kings subbasin, we suggest AEM as the optimal method to acquire the necessary subsurface data. Since Kings subbasin is a relatively huge subbasin with 3963 km² total surface area approximately stretching 70km in the north-south direction and 100km in the east-west direction, AEM, which can cover lands in terms of tens of kilometers, is suited to reveal the subsurface geology of the area. The primary objective of this survey is to detect the three major clay layers: A-clay (approximately 10m deep, 10m thick), C-clay (approximately 30m deep, 15m thick), and E-clay (Corcoran clay, approximately 130m deep, 15~60 m thick) (North Kings GSA, 106, North Fork Kings GSA, 136). Identifying and creating a detailed visualization of these near-surface clay layers are crucial to plan effective groundwater recharge in the subbasin.

We simulated to confirm the usefulness of the AEM method in detecting the three clay layers. We assumed the resistivity of sand and gravel as 35 ohm-m and clay as 15 ohm-m. The AEM's detectability of A-clay is 28%, C-clay is 25%, and E-clay is 13% (3-1), all well above the standard threshold of 3-5%. The DOI of the subbasin with a 3% error is 295m (3-2), which is enough to capture changes in resistivity to detect the three layers.



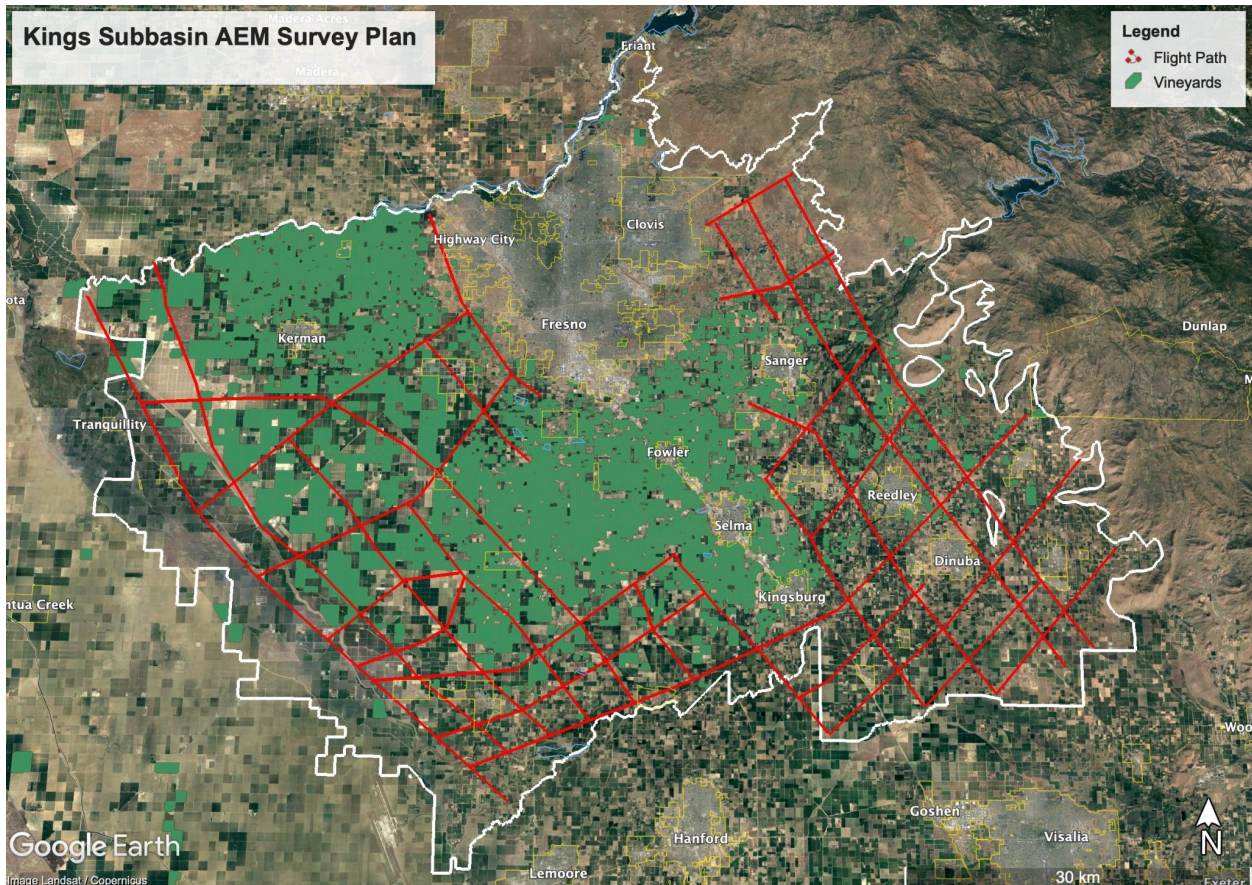
(3-1, Detectability regarding E-clay (Corocan Clay))



(3-2, DOI estimation with sand and gravel as 35 ohm-m and clay as 15 ohm-m)

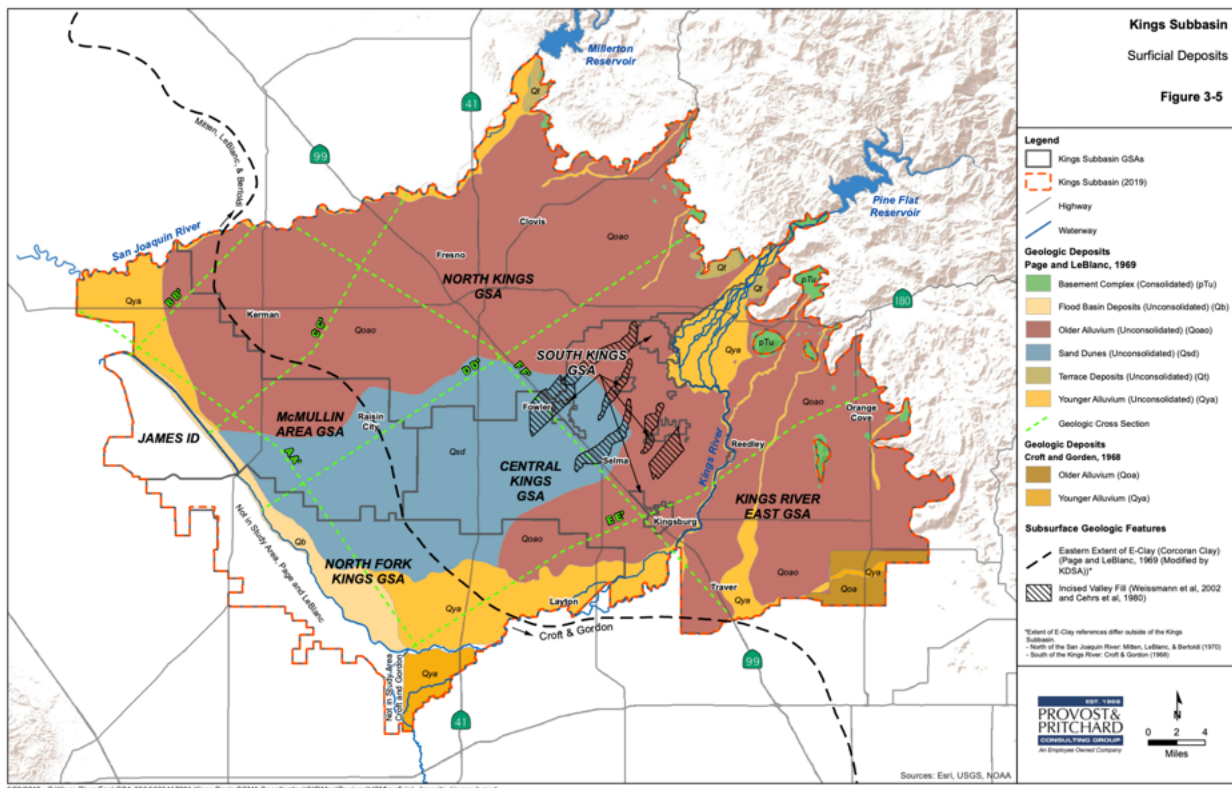
Kings Subbasin AEM Survey Plan

We suggest the survey plan as shown below (3-3). The red lines are the flight path of the helicopter towing the transmitter and receiver.



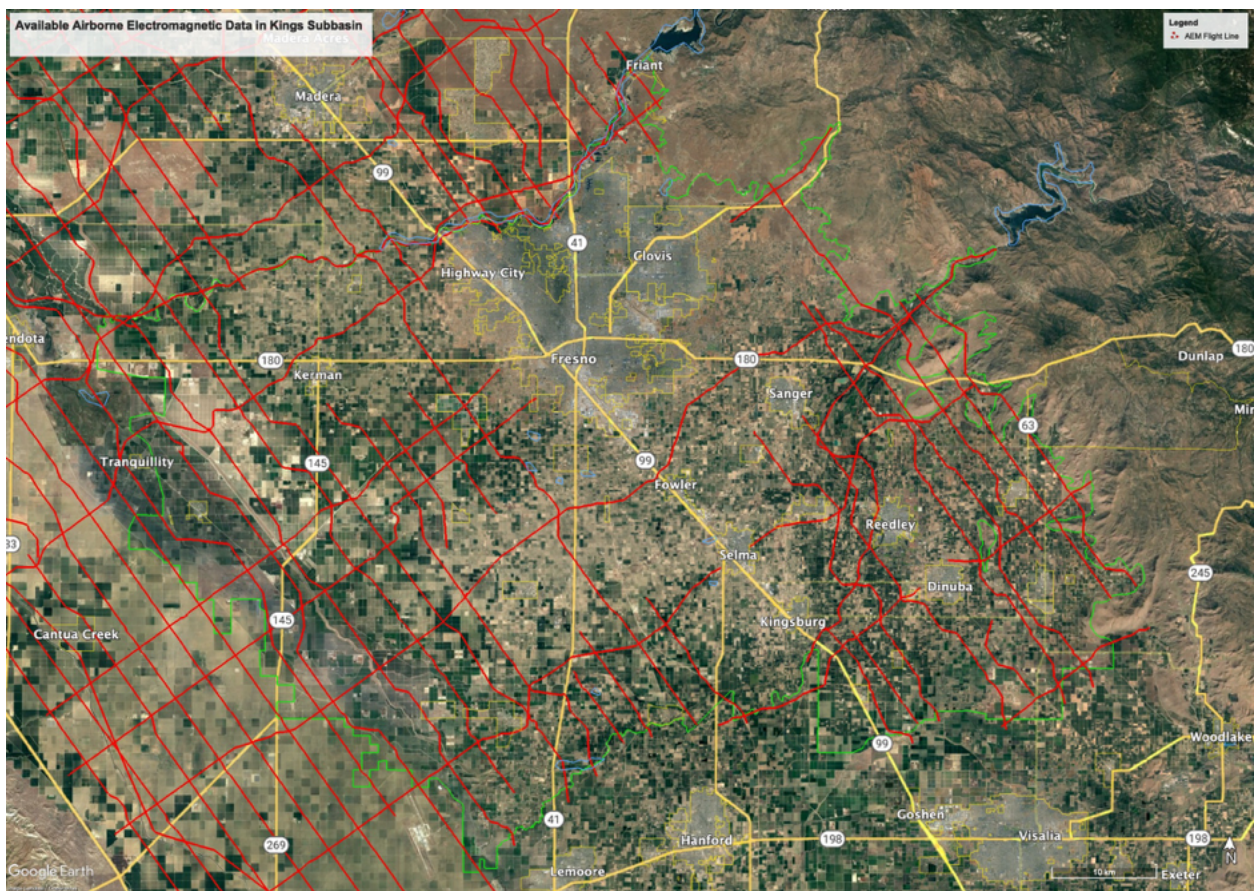
(3-3, AEM method survey plan)

Two major factors in deciding the flight path are the urban area, outlined with yellow, and the vineyards, colored in opaque green (MyGeodata Cloud). These surface structures can become noise to the EM data, making them less accurate. Urban areas are also not suited for flights in general. Since most of the Kings Subbasin belongs to Fresno County, one of the most urban but also agricultural areas in the San Joaquin Valley, flight paths will be quite limited. When crossing noises are inevitable, we wrote a path that crosses multiple noises (highways, vineyards, urban peripheries) at once to make the most use of the sacrifice of data. The pathway above covers the western part of the basin where the eastern extent of E-clay (Corcoran clay) is expected to exist, as the map below indicates.



(3-4, NKGSA 094, estimated eastern extent of E-clay (black dotted line))

4. Available Airborne Electromagnetic Data



(4-1, AEM Flight Line in Kings Subbasin)

AEM data from about 1260km of AEM flight lines are available in Kings Subbasin (DWR). The flight line is marked red on the map above. There are several constraints on the location of the flight line. One is urban areas. Kings Subbasin contains multiple major urban areas in the San Joaquin Valley, including the city of Fresno and Clovis. It can be inferred that flight lines avoided these areas due to safety reasons. Another factor is vineyards. Metal rods in vineyards can be noise to AEM surveys alongside highways and power lines. As we can see from 3-3 from the previous chapter, the flight line in 4-1 is sparse in the vineyard-dense areas in the south and west of Fresno.

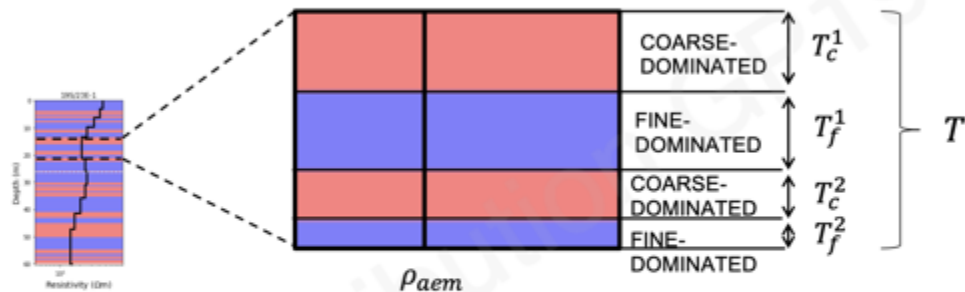
5. Developing the Relationship Between Resistivity and Sediment Type

Resistivity-to-sediment-type transformation

Through SEM survey and inversion, we are able to construct the 3-D resistivity map of the Kings Subbasin. In order to use this data to decide potential groundwater recharge location, we need to convert this 3-D resistivity data into 3-D sediment type data, which models the subsurface sediment type in Kings Subbasin. Different sediments typically have different resistivity, which allows us to infer the sediment type of a certain location and depth from its resistivity. However, this resistivity-sediment relation varies among sites, so we need to build a site-specific resistivity-to-sediment-type transform. This process takes the following steps, using the pre-existing well data.

1. Determine the collocation radius, and pair up well data (1-D sediment type log) with AEM data if available within the collocation radius.
2. For each pair, find a certain range of depth that has a single resistivity and several sediment types. For example, look at the section with thickness T in Figure 5-1 (Knight). The total resistivity of the section (ρ_{em}) is available from the AEM data. At the same time, by referring to the well data, we can observe that this section consists of two coarse-dominated (sand&gravel) layers and two fine-dominated (clay) layers, each with unknown resistivity ρ_c and ρ_f . By using the parallel-circuit model (equation A), we acquire an equation that can be used to solve for ρ_c and ρ_f .

**Select one cell (thickness T) in 1D resistivity model
and corresponding section of 1D sediment-type log**



Use parallel-circuit model to approximate EM measurement

Equation A

$$\rho_{em}^{-1} = \rho_c^{-1} \left(\frac{T_c^1}{T} + \frac{T_c^2}{T} \right) + \rho_f^{-1} \left(\frac{T_f^1}{T} + \frac{T_f^2}{T} \right)$$

ρ_{em} : EM resistivity value in a cell of 1D resistivity model

ρ_c : Unknown resistivity of COARSE-DOMINATED

ρ_f : Unknown resistivity of FINE-DOMINATED

(5-1, Knight, Example of a co-located 1-D resistivity model and 1-D sediment type log)

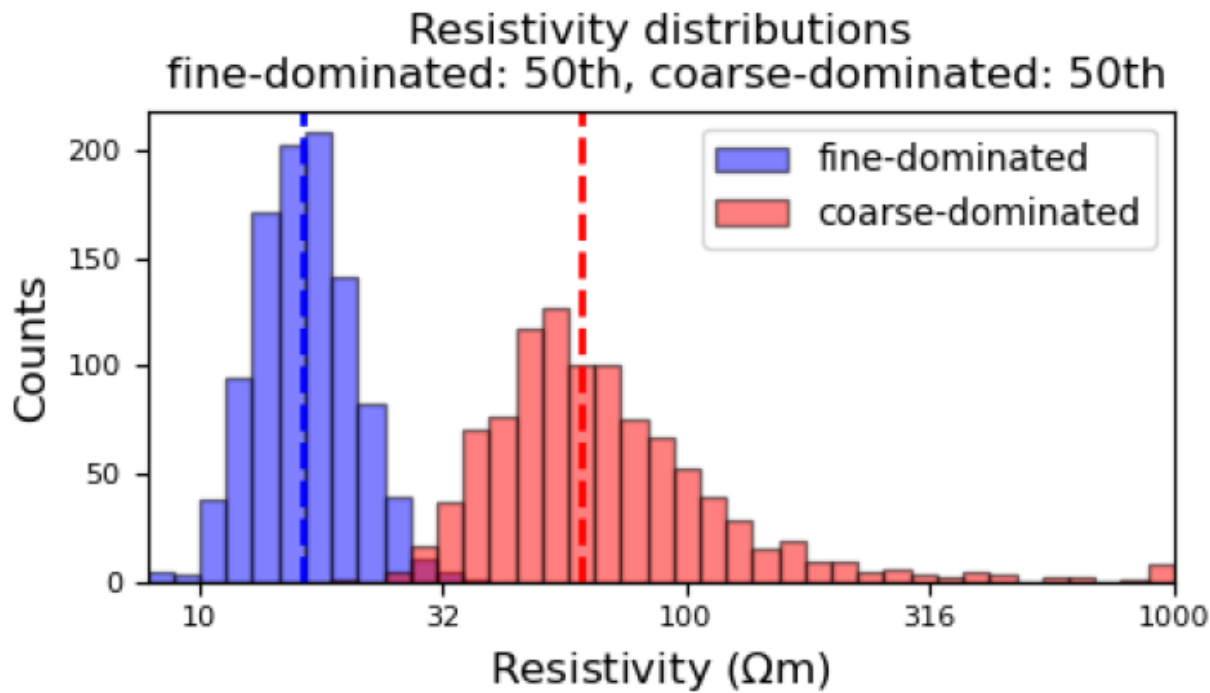
3. By repeating this for all the well-data-AEM-data pairs, we accumulate equations of ρ_c and ρ_f . Finally, we solve these equations for ρ_c and ρ_f with bootstrapping, ending up with a histogram of estimated resistivity for both coarse-dominated and fine-dominated sediments.

Different collocation-radius will vastly change the number and quality of equations we get, affecting the result of this transformation. In the section below, we conducted the transformation in Kings Subbasin with varying collocation radii to determine its optimal value.

Simulation

Below is the number of collocated wells and a histogram of resistivity distribution derived by the process 1 to 3 above with different collocation radii. The value of the collocation radius and the number of driller's logs available are listed on the upper left of each graph. The median for both fine-dominated and coarse-dominated resistivity is listed below each graph.

50m, 42 collocated wells



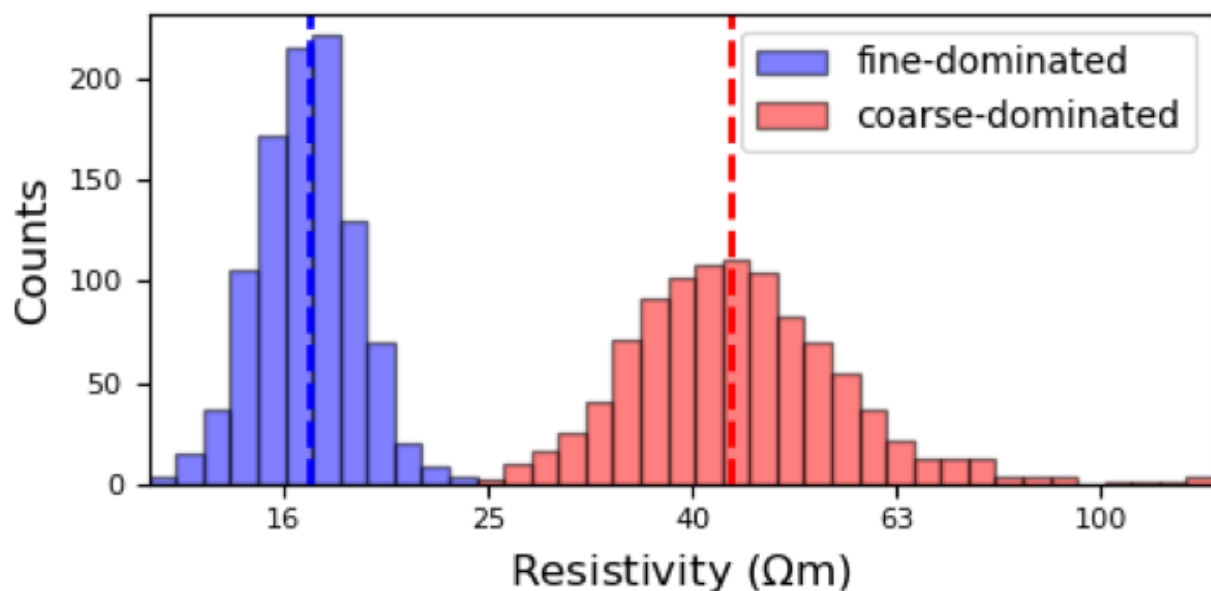
(5-2, resistivity distribution with 50m collocation radius)

Median fine-dominated: 16.3, coarse-dominated: 60.8

Observation: Overlap between two sediments, unrealistic difference in resistivity

100m, 139 collocated wells

Resistivity distributions fine-dominated: 50th, coarse-dominated: 50th



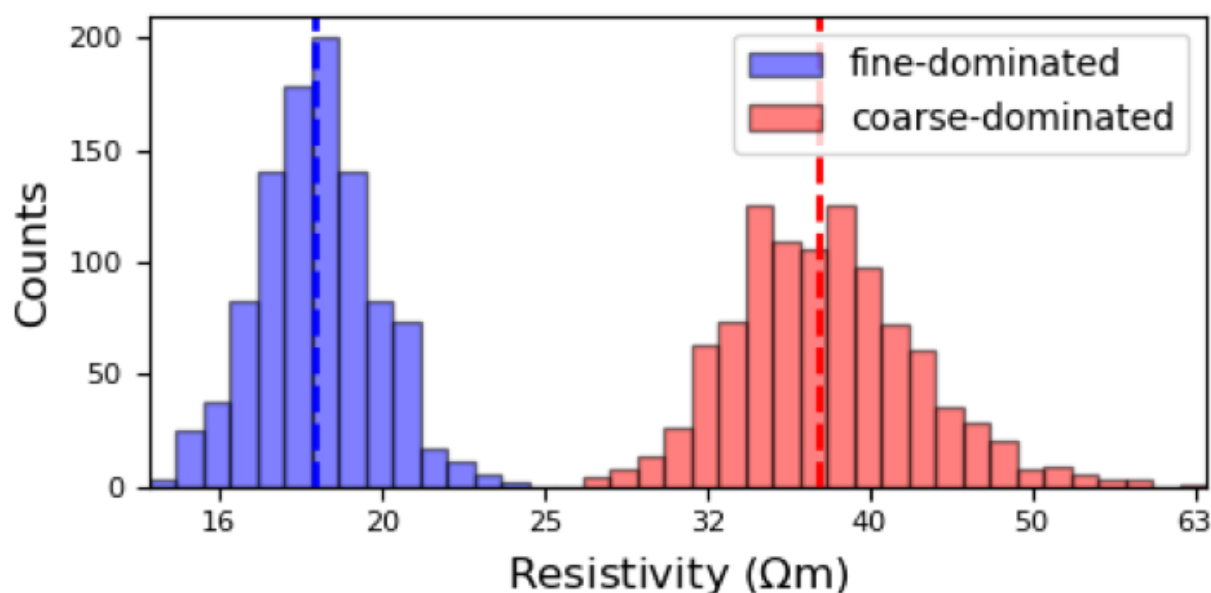
(5-3, resistivity distribution with 100m collocation radius)

Median fine-dominated: 16.7, coarse-dominated: 43.3

Observation: Slight overlap between two sediments, large difference in resistivity

150m, 205 collocated wells

Resistivity distributions fine-dominated: 50th, coarse-dominated: 50th

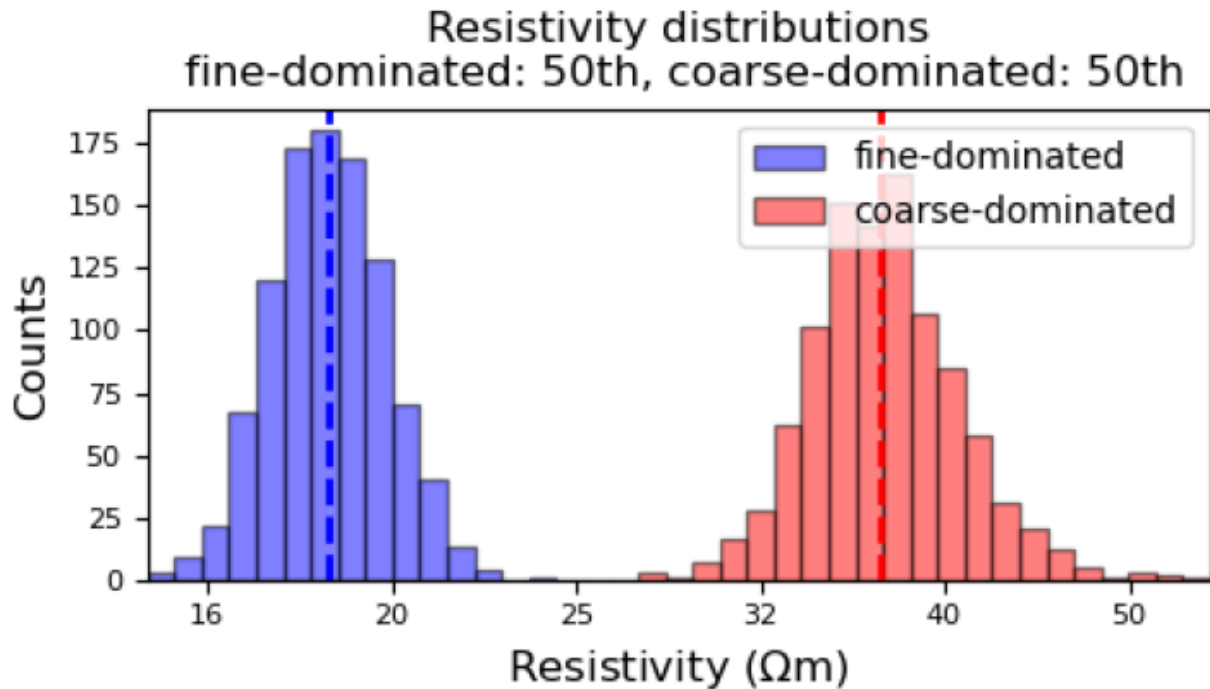


(5-4, resistivity distribution with 150m collocation radius)

Median fine-dominated: 18.1, coarse-dominated: 37.0

Observation: Non-uniform histogram shape for coarse-dominated

200m, 316 collocated wells



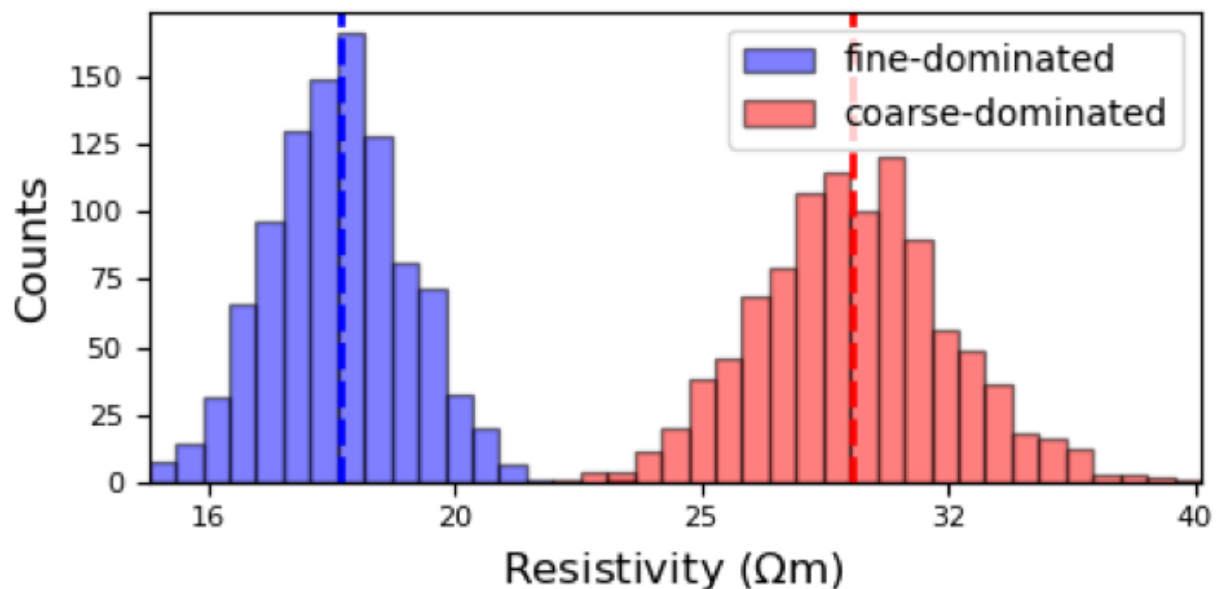
(5-5, resistivity distribution with 200m collocation radius)

Median fine-dominated: 18.3, coarse-dominated: 36.7

Observation: No overlap, ideal distance between two resistivity

300m, 524 collocated wells

Resistivity distributions fine-dominated: 50th, coarse-dominated: 50th



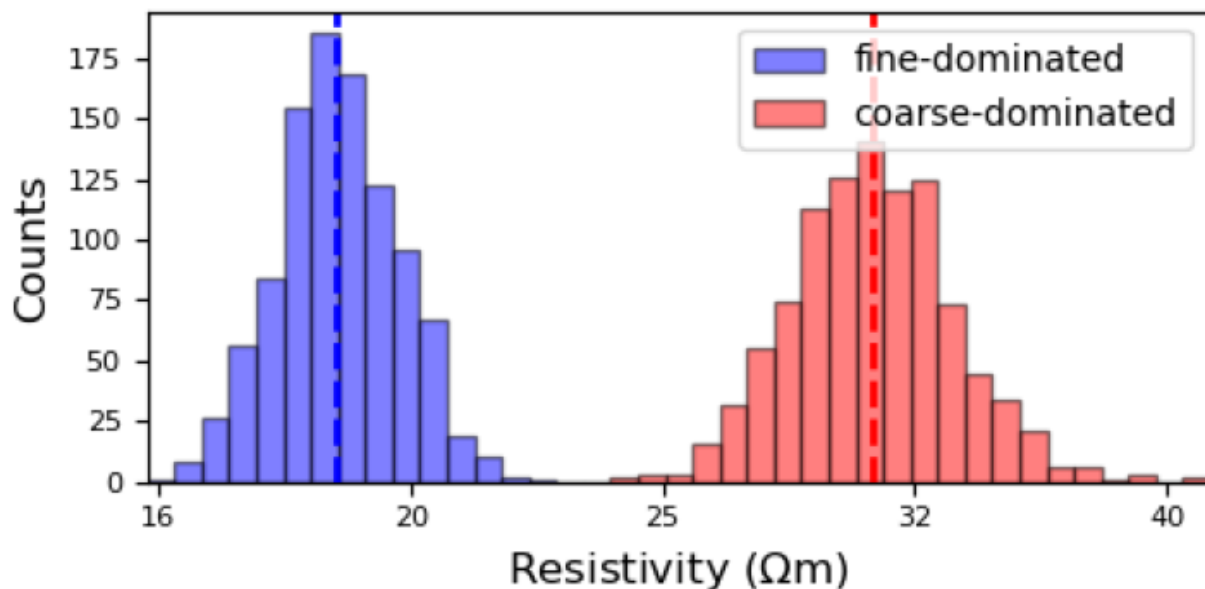
(5-6, resistivity distribution with 300m collocation radius)

Median fine-dominated: 17.9, coarse-dominated: 28.8

Observation: Small distance between resistivity

400m, 722 collocated wells

Resistivity distributions fine-dominated: 50th, coarse-dominated: 50th



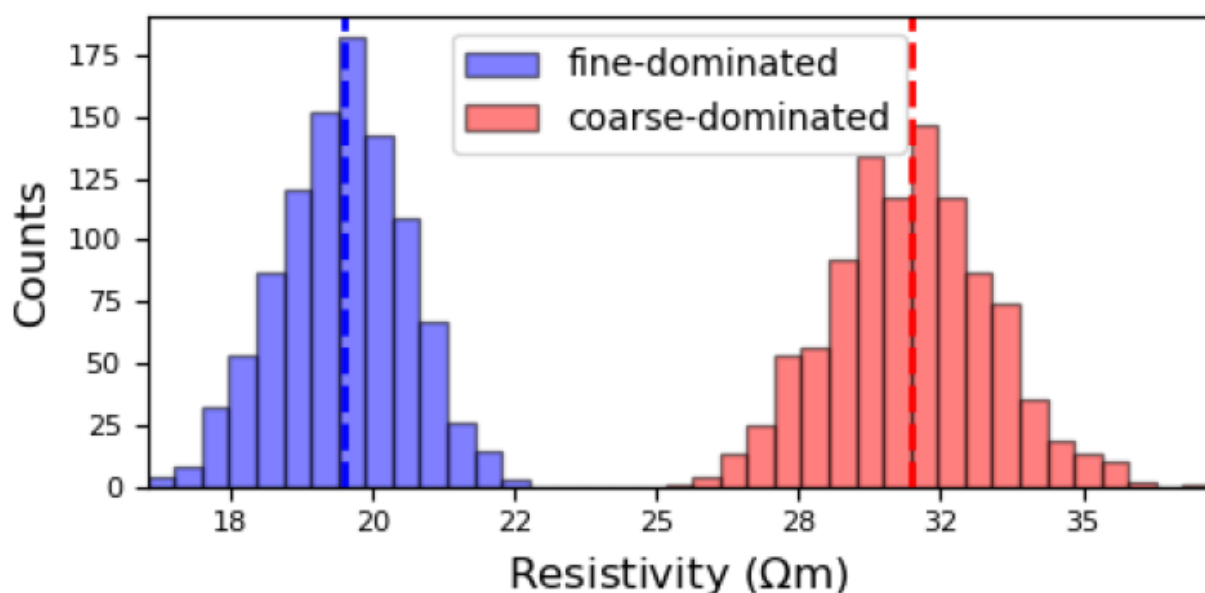
(5-7, resistivity distribution with 400m collocation radius)

Median fine-dominated: 18.6, coarse-dominated: 30.4

Observation: Small difference in resistivity

500m, 930 collocated wells

Resistivity distributions fine-dominated: 50th, coarse-dominated: 50th

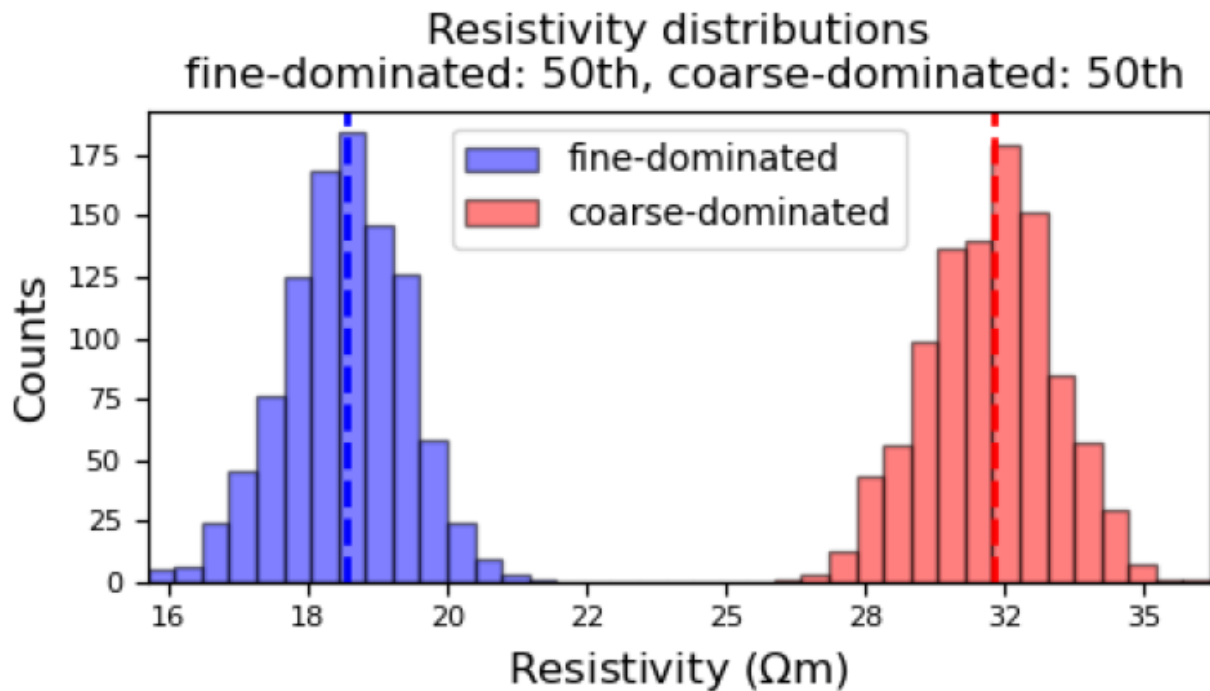


(5-8, resistivity distribution with 500m collocation radius)

Median fine-dominated: 19.4, coarse-dominated: 30.8

Observation: Small difference in resistivity, unrealistic collocation radius (assumption that geology is homogenous within 500m distance)

750m, 1378 collocated wells

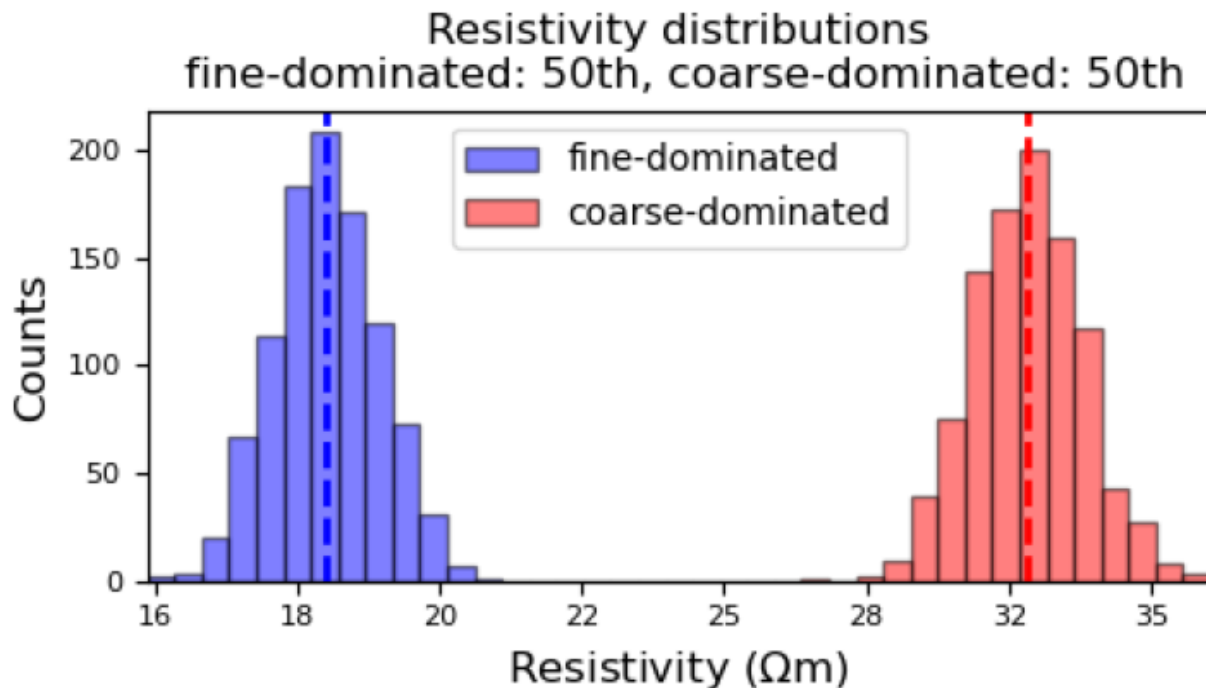


(5-9, resistivity distribution with 750m collocation radius)

Median fine-dominated: 18.3, coarse-dominated: 31.3

Observation: Unrealistic collocation radius (assumption that geology is homogenous within 750m distance)

1km, 1767 collocated wells

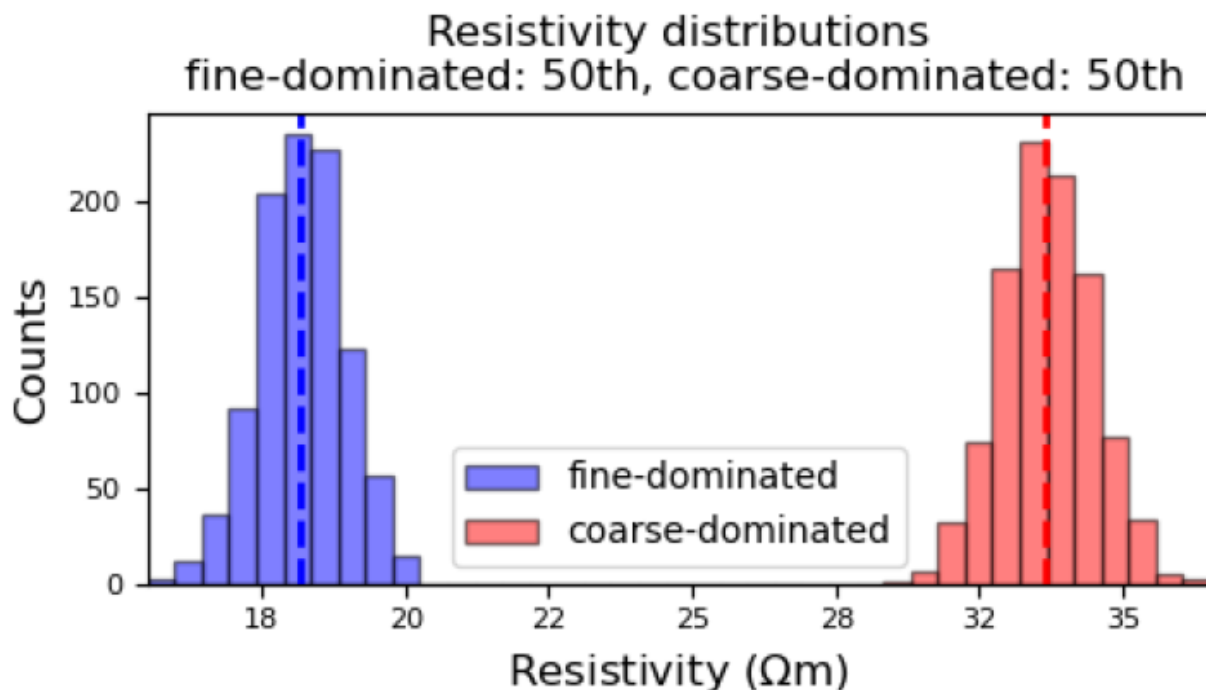


(5-10, resistivity distribution with 1km collocation radius)

Median fine-dominated: 18.1, coarse-dominated: 32.1

Observation: Unrealistic collocation radius (assumption that geology is homogenous within 1km distance)

2km, 2821 collocated wells

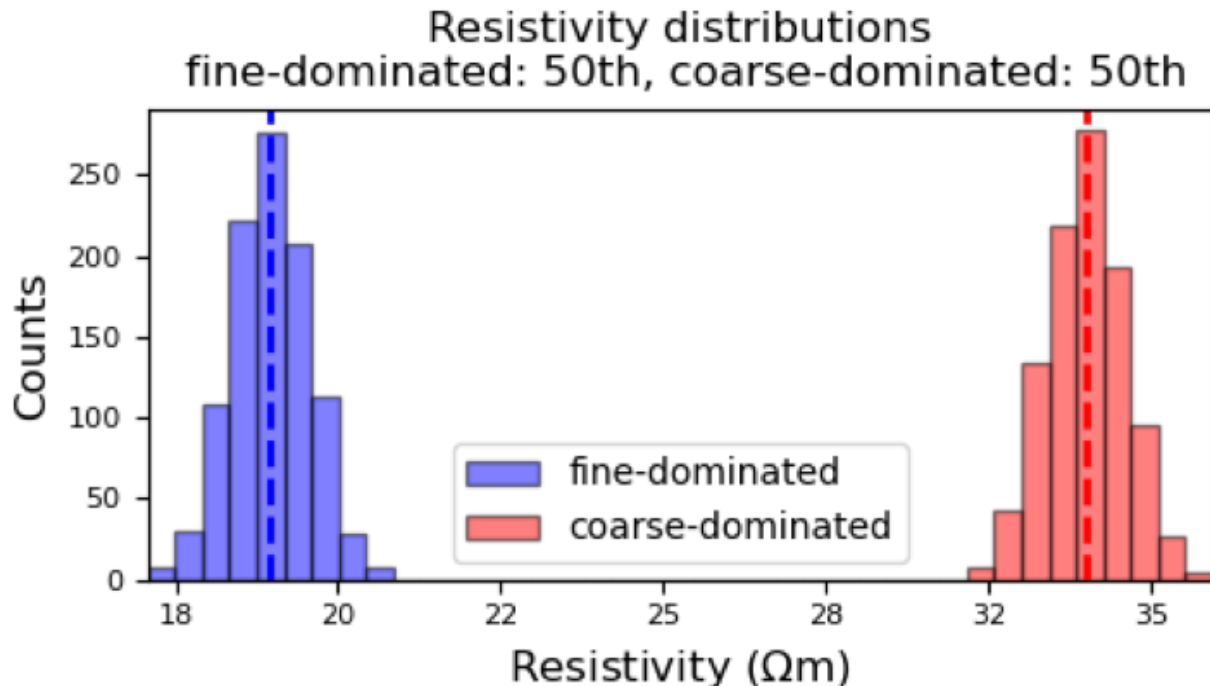


(5-11, resistivity distribution with 2km collocation radius)

Median fine-dominated: 18.3, coarse-dominated: 33.3

Observation: Unrealistic collocation radius (assumption that geology is homogenous within 2km distance)

5km, 3837 collocated wells



(5-12, resistivity distribution with 5km collocation radius)

Median fine-dominated: 19.0, coarse-dominated: 33.8

Observation: Unrealistic collocation radius (assumption that geology is homogenous within 5km distance)

Result

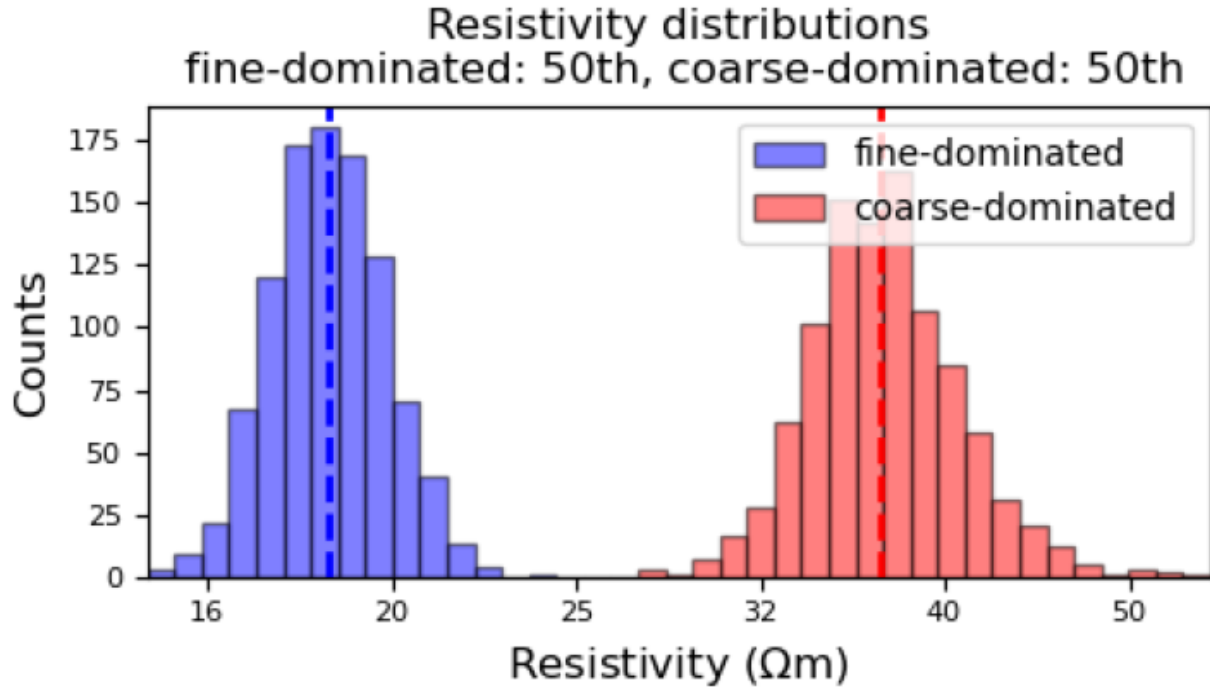
Based on the simulations above, we propose 200m as the collocation radius. With scarce overlapping between coarse and fine sentiments, close-to-normal distribution of each sediment, and 18.4 ohm-m difference between median coarse and fine-dominated resistivity difference, 200m is enough to distinguish two sediment types but not overshooting.

6. Developing the Transform from Resistivity to Fraction Coarse-Dominated

Resistivity to Fraction Coarse-Dominated Transform

Now that we developed a local resistivity distribution in the last section, we can define the transformation between resistivity and the fraction of coarse-dominated material. For reference, below (6-1) is the distribution of resistivity in the Kings subbasin developed with a 200m collocation radius.

200m, 316 collocated wells



(6-1, resistivity distribution with 200m collocation radius)

Median fine-dominated: 18.3, coarse-dominated: 36.7

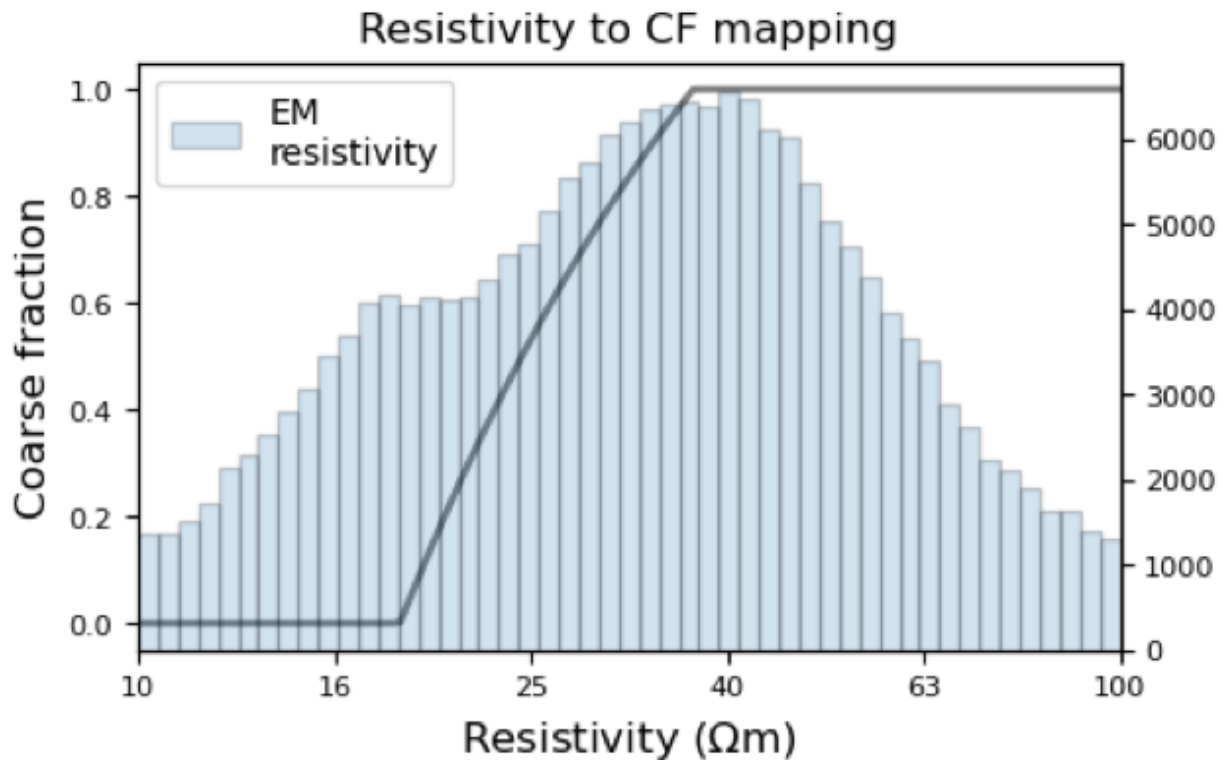
It is safe to assume that for resistivity less than 18.3 (median of fine-dominated), it is 0% coarse-dominated (100% fine-dominated), and for resistivity larger than 36.7 (median of coarse-dominated), it is 100% coarse-dominated. For the resistivity between 18.3 and 36.7, where fine and coarse sediments are likely to co-exist, we need to calculate the approximate fraction of coarse-dominated. Let the target resistivity ρ_{em} ($18.3 < \rho_{em} < 36.7$), coarse-dominated resistivity ρ_c , fine-dominated resistivity ρ_f , and the fraction coarse-dominated FCD. We can establish the following equation between these parameters (6-2).

$$\rho_{em}^{-1} = \rho_c^{-1}FCD + \rho_f^{-1}(1 - FCD)$$

(6-2, Relationship between four parameters)

We can plug in 18.3 (median of fine-dominated) as ρ_f and 36.7 (median of coarse-dominated) as ρ_c and solve for FCD, since they are the most likely values for ρ_f and ρ_c locally. By solving this equation with

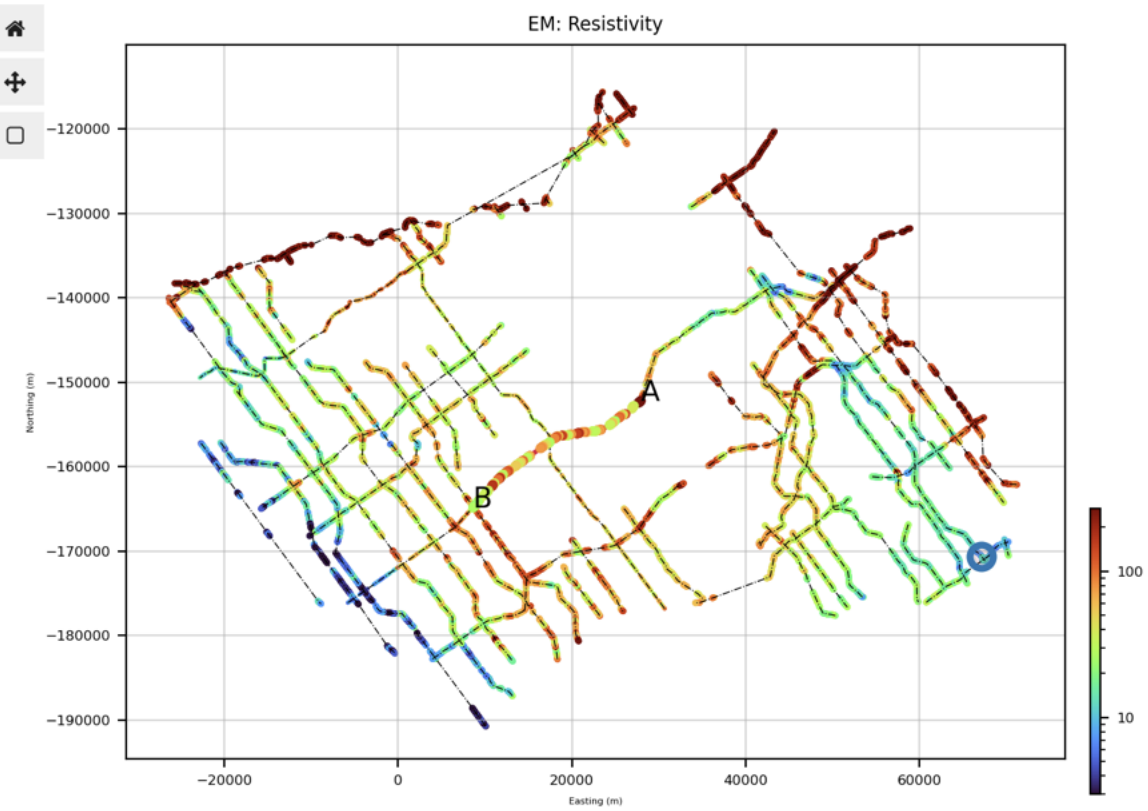
multiple values of ρ_{em} , we can plot the fraction coarse-dominated as the grey line in the graph below (6-3).



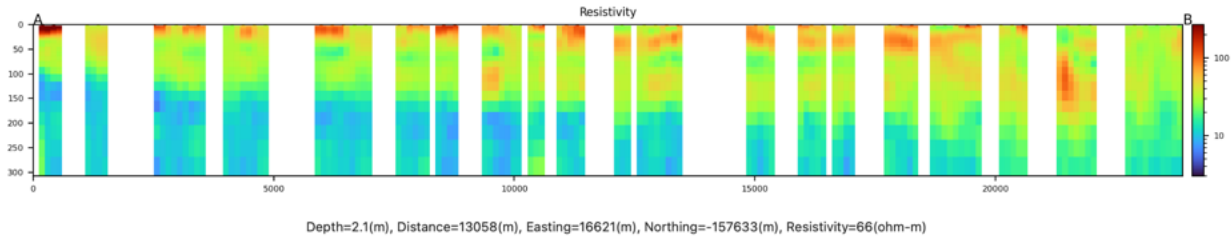
(6-3, Resistivity transform plot, generated by *fastpath*)

7. Developing a Model of Sediment Type

As we discussed in Chapter 3, by inverting the collected AEM data, we are able to obtain a 1-D resistivity model. Below is an example of a 1-D resistivity model based on the AEM data offered by the DWR AEM survey (DWR) (7-1, 7-2).

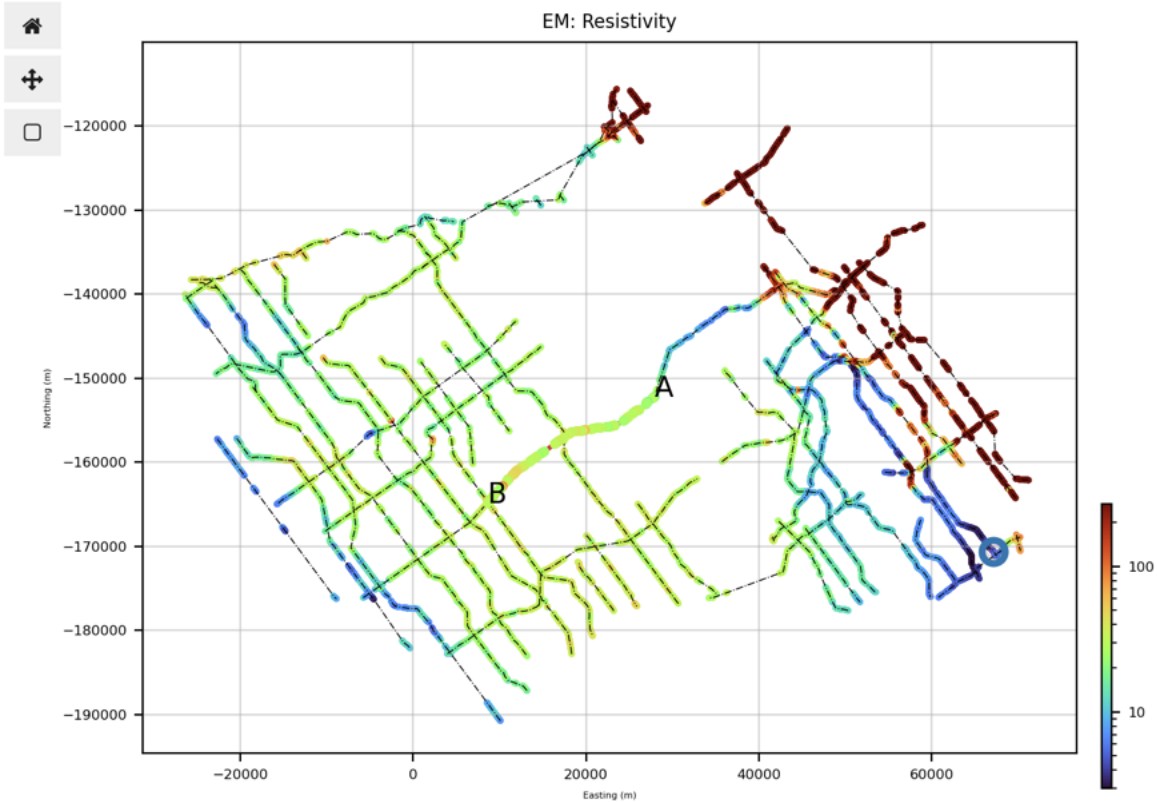


(7-1, Planar view of resistivity in Kings Subbasin, generated by *fastpath*)



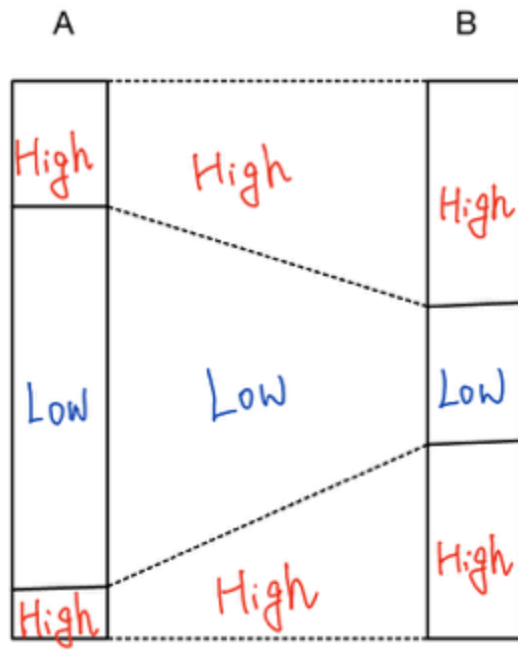
(7-2, Subsurface resistivity of A-B cut, generated by *fastpath*)

7-1 is a planar view of the resistivity at the surface (depth 0m) in Kings Subbasin. Blue is low resistivity, and red is high resistivity. The high resistivity (dark red) in the eastern part of the subbasin is likely to be bedrock. 7-2 is the resistivity model of the subsurface at the A-B cut in 7-1. Note that the position of A-B is inverted in 7-2. This informs us that there's a general trend of resistivity decreasing as depth increases along the A-B cut. We are also able to provide planar views in various depths. 7-3 is a basin-wide view of resistivity at 15m depth. The central to the eastern part of the subbasin generally has low resistivity at 15m depth than at the surface, from which we can infer the existence of A-clay.



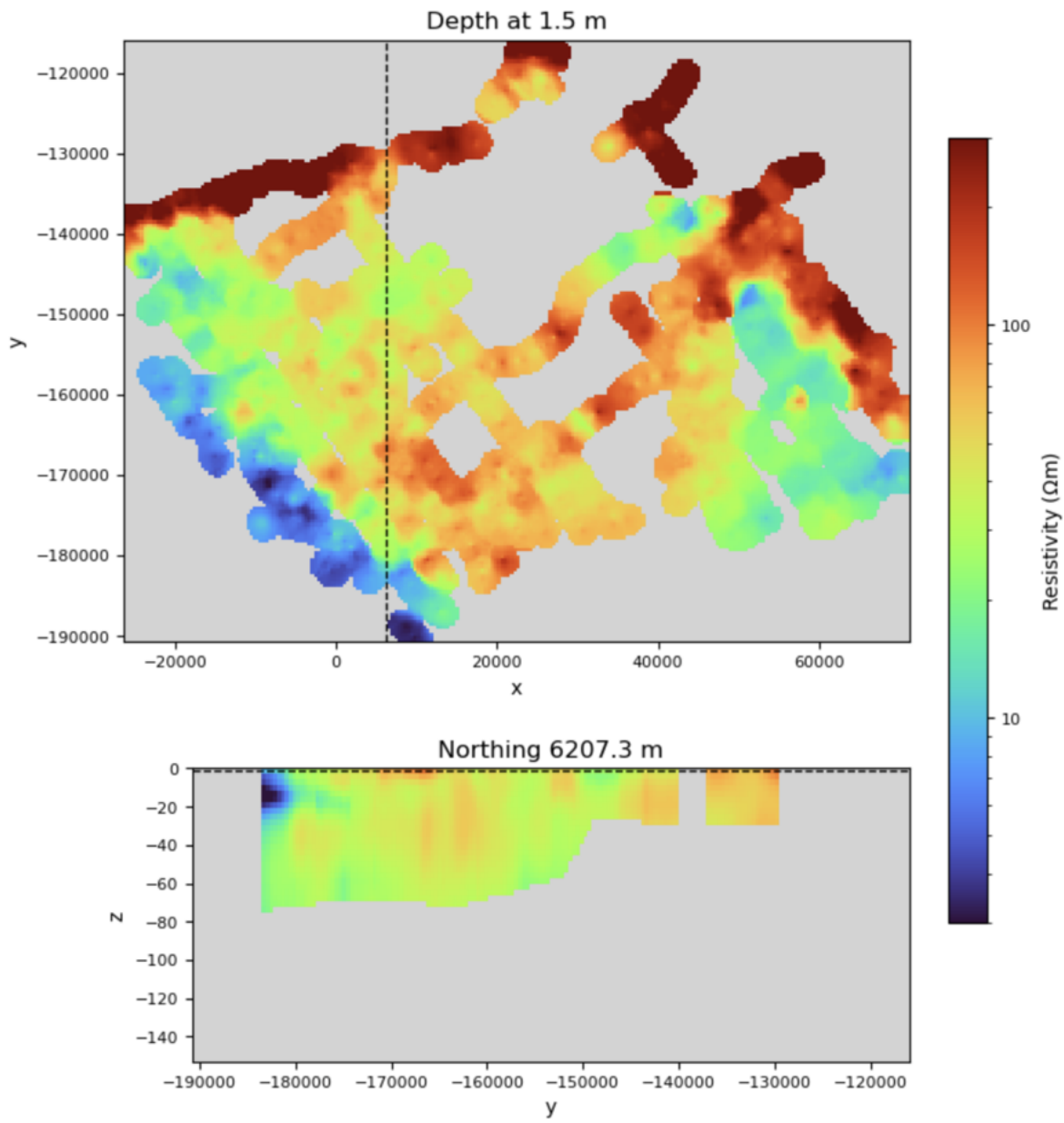
(7-3, Planar view of resistivity at 15m depth in Kings Subbasin, generated by *fastpath*)

However, all the 1-D resistivity models above are merely a model of the resistivity of the grounds below the flight paths. We need to conduct interpolation on this to acquire the 3-D resistivity model of Kings Subbasin. Interpolation is simply done by connecting the layers with direct lines between two points (7-4), although the actual calculation is more complicated as resistivity values are continuous. Interpolation is not conducted when a certain location is more than 2km away from the closest 1-D resistivity data.



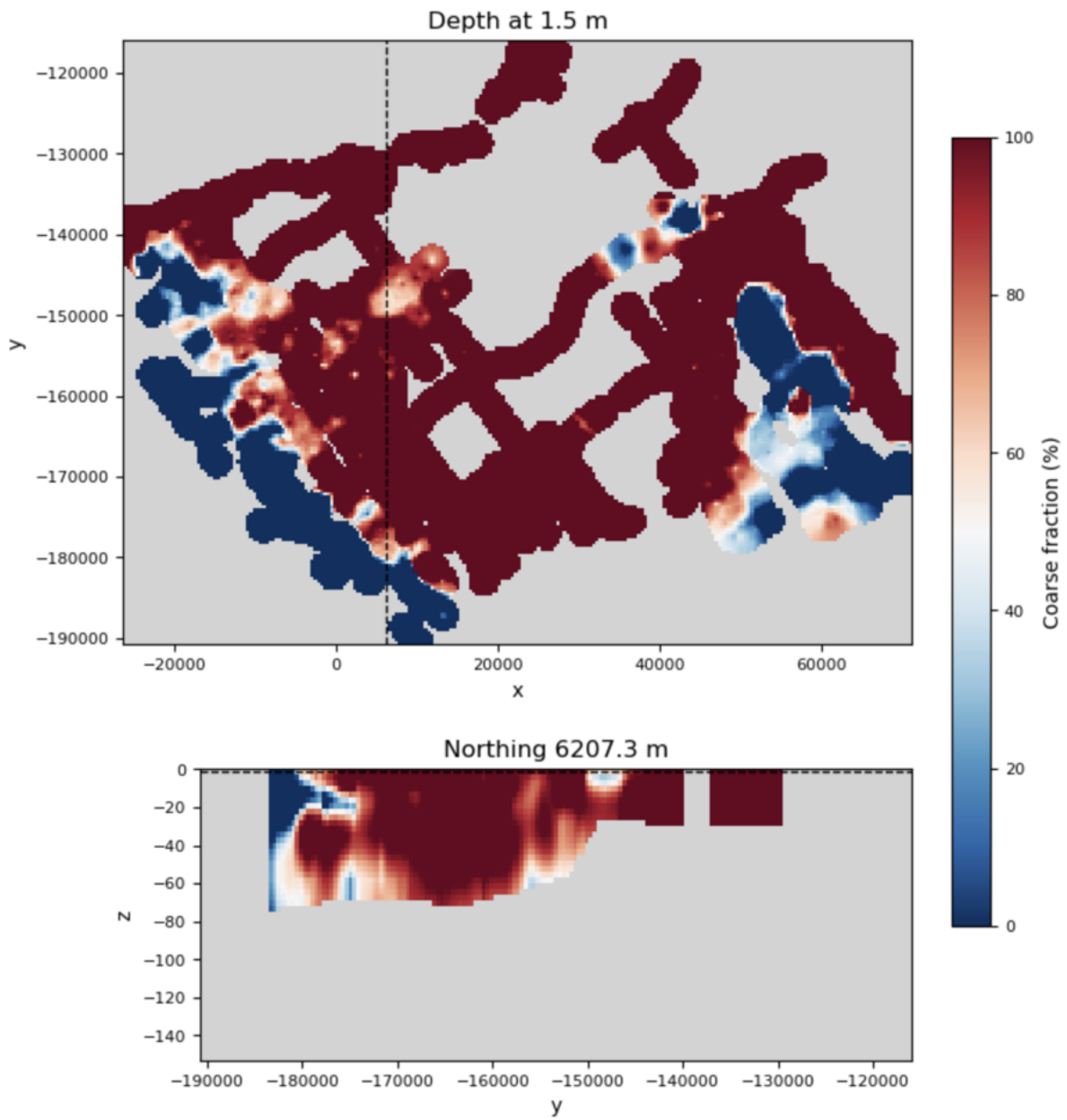
(7-4, Simplified image of interpolation)

The resulting 3-D resistivity model is below (7-5). The image above is the subbasin-wide planar view of resistivity at 1.5m depth, and the image below is the subsurface resistivity at the black-dotted-line cut. In comparison with 7-1, we can see how estimated resistivity is now available in various locations across the basin, although places more than 2km away from the original lines are left blank.



(7-5, interpolated 3-D resistivity model of Kings Subbasin, generated by *fastpath*)

Finally, based on the transform between resistivity and fraction of coarse-dominated material we defined in Chapter 6, we can generate a 3-D model of fraction coarse-dominated (7-6).

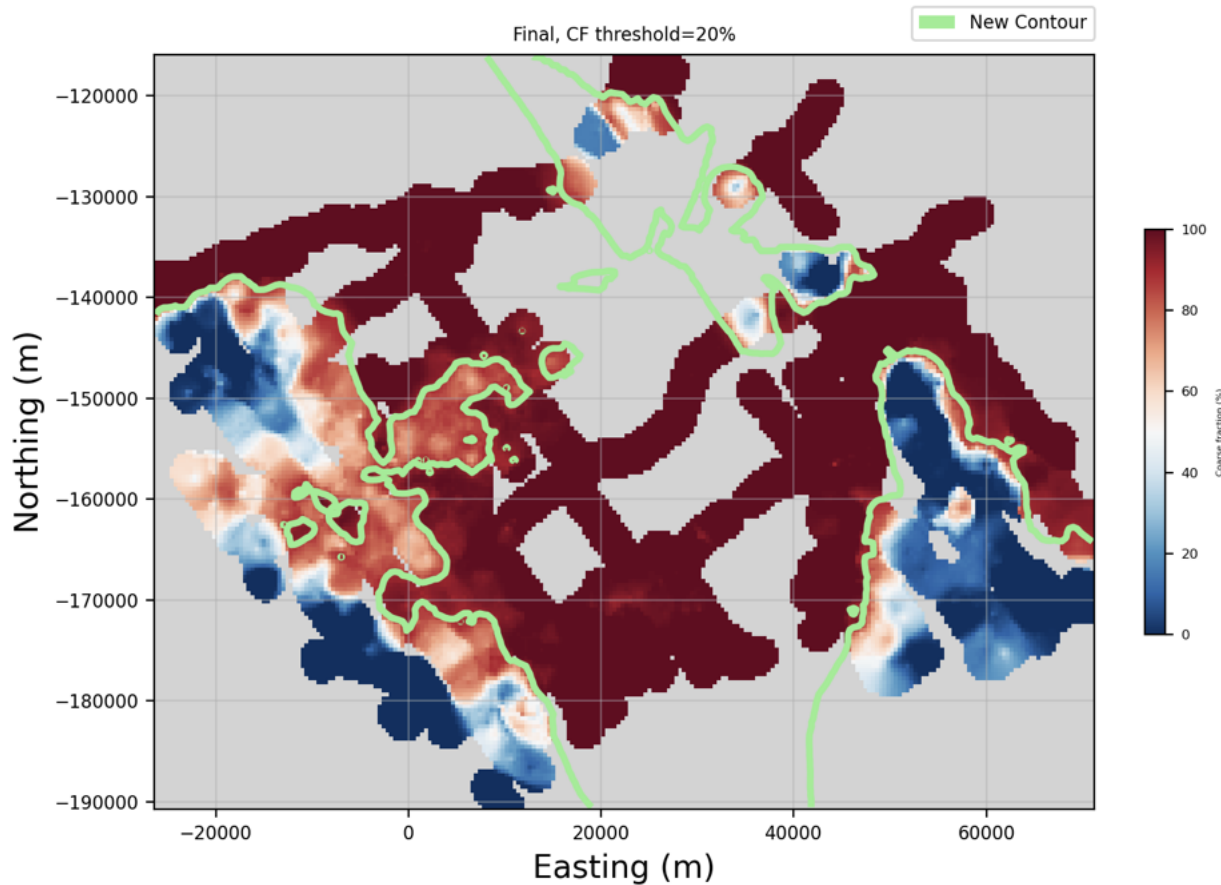


(7-6, 3-D fraction coarse-dominated model of Kings Subbasin, generated by *fastpath*)

8. Evaluation for Recharge - Metric 1

The first metric we will use to evaluate recharge potential based on the fraction coarse-dominated model is the integrated fraction of coarse-dominated at a given location. The result is shown below (8-1). This metric gives the overall fraction of coarse-dominated in the unsaturated zone of a given location. For example, the overall fraction of coarse-dominated at point (easting = -20000, northing = -160000) is about

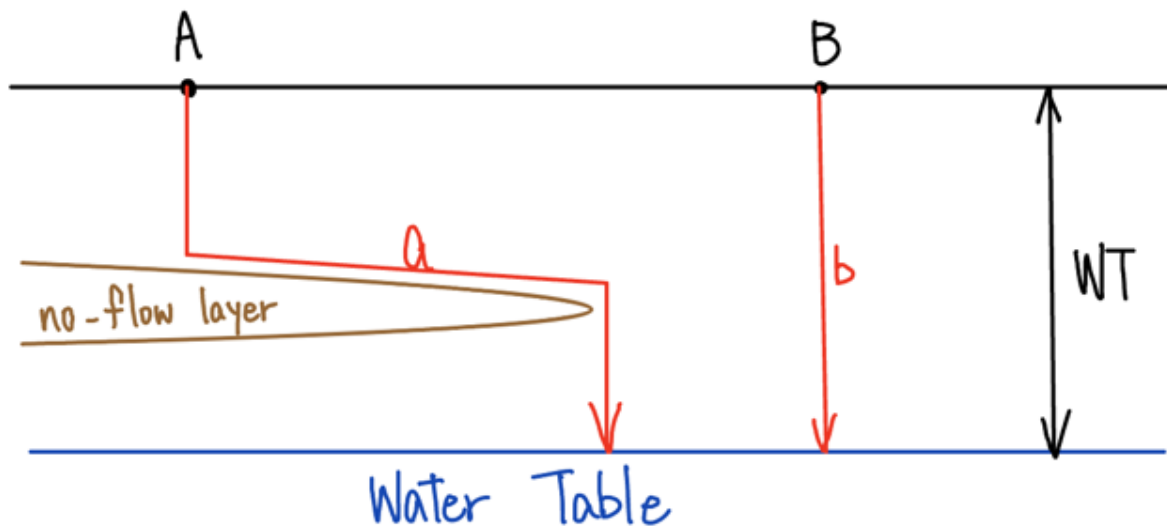
70%, which is why it's colored light red. The green line is the contour plot of the fraction coarse-dominated = 90%. We can assume that the southeast and southwest part of the basin is mainly fine-dominated, while other parts are coarse-dominated and thus suited for recharge. However, this metric is not decisive since it does not account for the distribution of coarse and fine sediments in a given subsurface. For example, even if a certain location is 90% coarse-dominated, it is not suited for recharge if 10% of fine sediments are accumulated on the surface level.



(8-1, Integrated fraction of coarse-dominated with 90% contour plot, generated by *fastpath*)

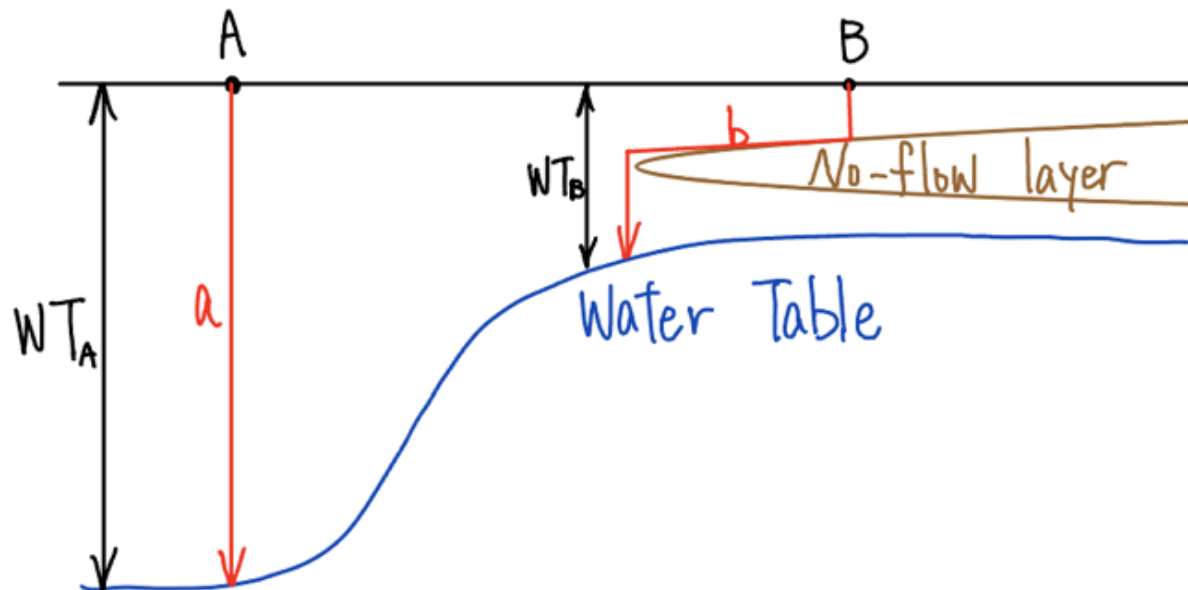
9. Evaluation for Recharge Metric 2

Another metric we can use to evaluate recharge potential is the shortest path length from the surface to the water table. Consider a subsurface as below (9-1) with two potential recharge locations, A and B.



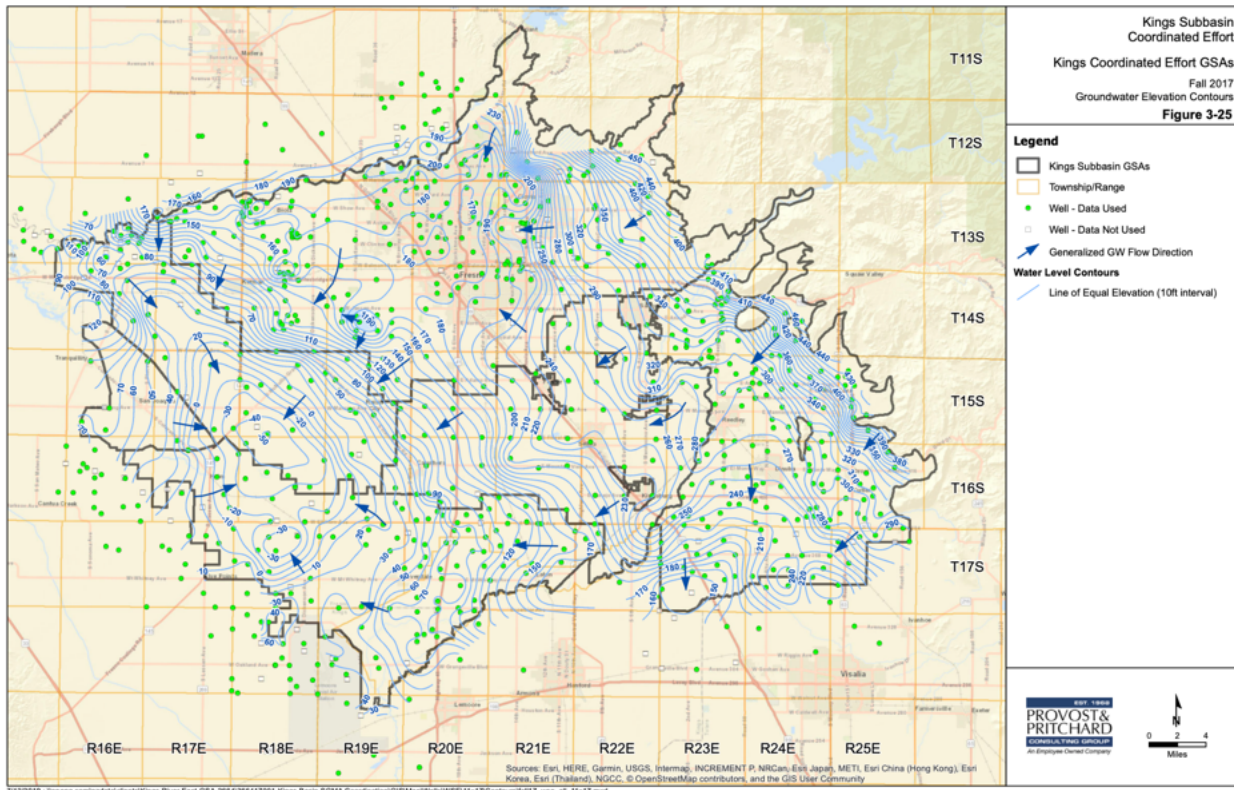
(9-1, Path length)

There is a no-flow layer (a layer through which water cannot flow) directly below point A, so in order to successfully reach the water table, the water supplied to point A needs to take a detour around the no-flow layer (path a). On the other hand, water provided to point B can directly reach the water table (path b). Therefore we can infer from the path length ($b < a$) that location B is more suited for a recharge if we want to reach the water table as quickly as we can. However, the path length is not as useful when the target area has varying water tables, and we do not prioritize minimizing the time to reach the water table. Consider another subsurface as below (9-2).



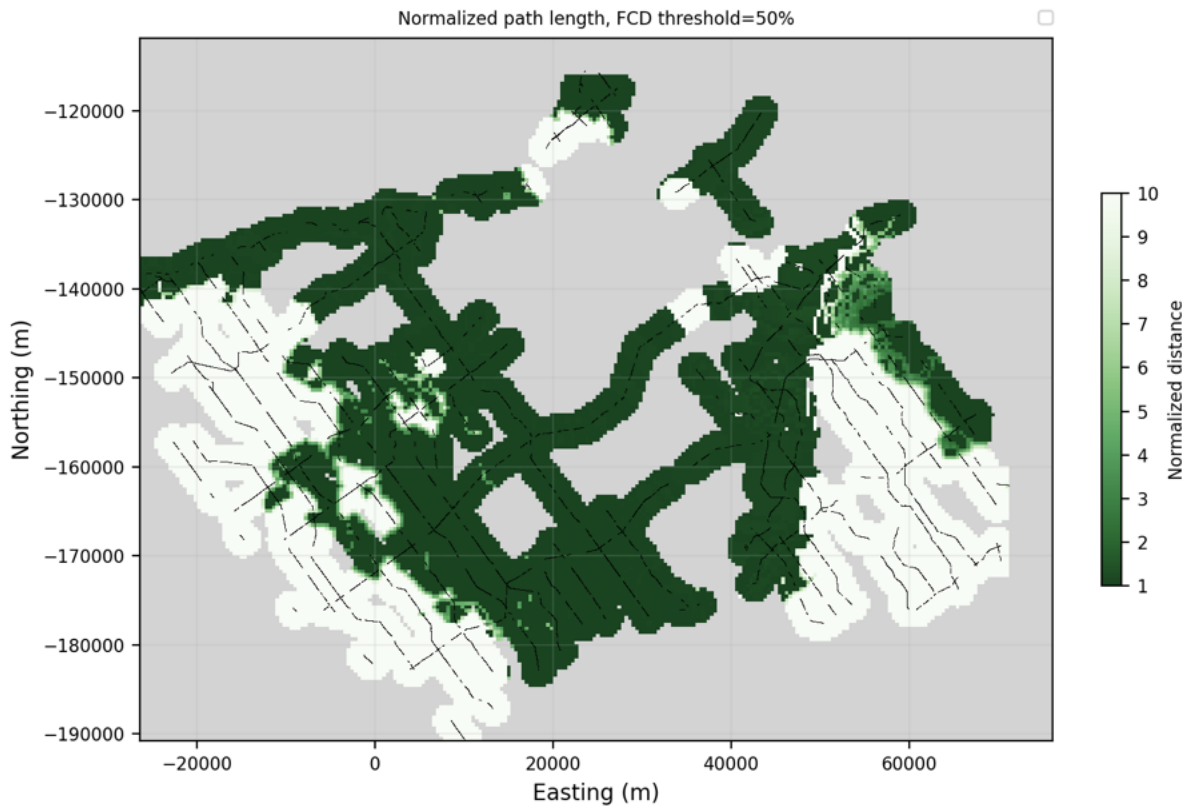
(9-2, Normalized path length)

If we just compare the path length, it seems like B is a better recharge location since $b < a$. However, this is merely because the water table is much near-surface closer at point B. If we do not put emphasis on reaching the water table quickly, location A is also a strong candidate with a straight path to the water table. Therefore we divide the path length by the depth of the water table to get a **normalized path length**. Although A has a longer path length ($a > b$), it has a shorter normalized path length ($a/\text{WT}_a < b/\text{WT}_b$). The normalized path length is essentially the efficiency of recharging depth. Since Kings Subbasin has varying water tables over the basin (9-3), we suggest the normalized water table as a more reliable metric.



(9-3, North Kings GSP, 135, Water table contour plot of Kings Subbasin)

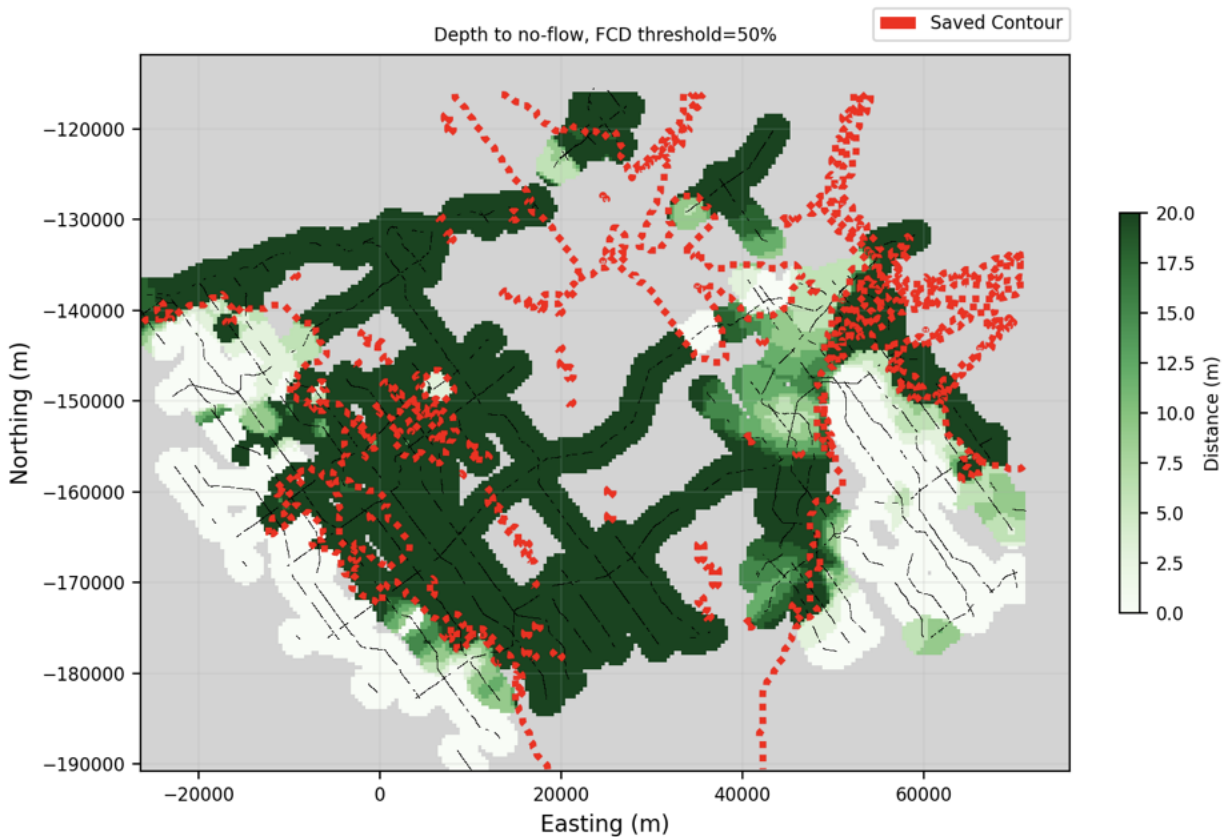
Before implementing this metric, we need to decide the threshold for a no-flow layer. In Chapter 7, we generated a 3-D model of fraction coarse-dominated to get a general sense of water transportability. Now, we need to determine which part of this model should be considered as "no-flow" when calculating normalized path length. In this report, we would use 50% as the threshold, which means that it is considered "no-flow" if the fraction coarse-dominated is below 50%. This is a relatively strict threshold (even if a certain grid is 49% coarse-dominated, we assume that water does not flow through it), which allows us to sort out potential recharge sites efficiently. The result is shown below (9-4). We can observe a general trend of the central subbasin having a normalized path length close to 1 while the eastern and western parts of the basin are hard to reach the water table.



(9-4, Normalized path length with FCD threshold = 50%, generated by *fastpath*)

10. Evaluation for Recharge Metric 3

The third metric we introduce is the depth of a unit that has been designated as no-flow (either the water table or units with fraction coarse-dominated below threshold). In the previous chapter, we determined below 50% fraction coarse-dominated as no-flow. It is important to grasp the depth of the closest no-flow unit from the surface when assessing a recharge site, as this depth gives us a sense of where the water might stick around in the short term after recharge. For example, if we recharge a location with a 5m depth of a unit that has been designated as no-flow, there will be water extremely close to the surface for a while, increasing the risk of flooding. This is detrimental to various crops grown in our basin, such as almonds, as it might lead to root loss and, ultimately, tree loss. Thus, we want to avoid recharging locations with shallow depths of a unit that has been designated as no-flow. Since this metric is more about predicting the negative impact after recharge rather than estimating the recharge potential, it is not suited for sorting out the recharge location itself, but it is useful for "double-checking" the locations sorted by the previous metrics. The map below shows the depth of no-flow units in Kings Subbasin (10-1). The red dotted line is the contour plot of normalized path length = 2.01. We can see that some parts of the basin with preferable normalized path length actually might not be suited for recharge due to shallow depth to no-flow.

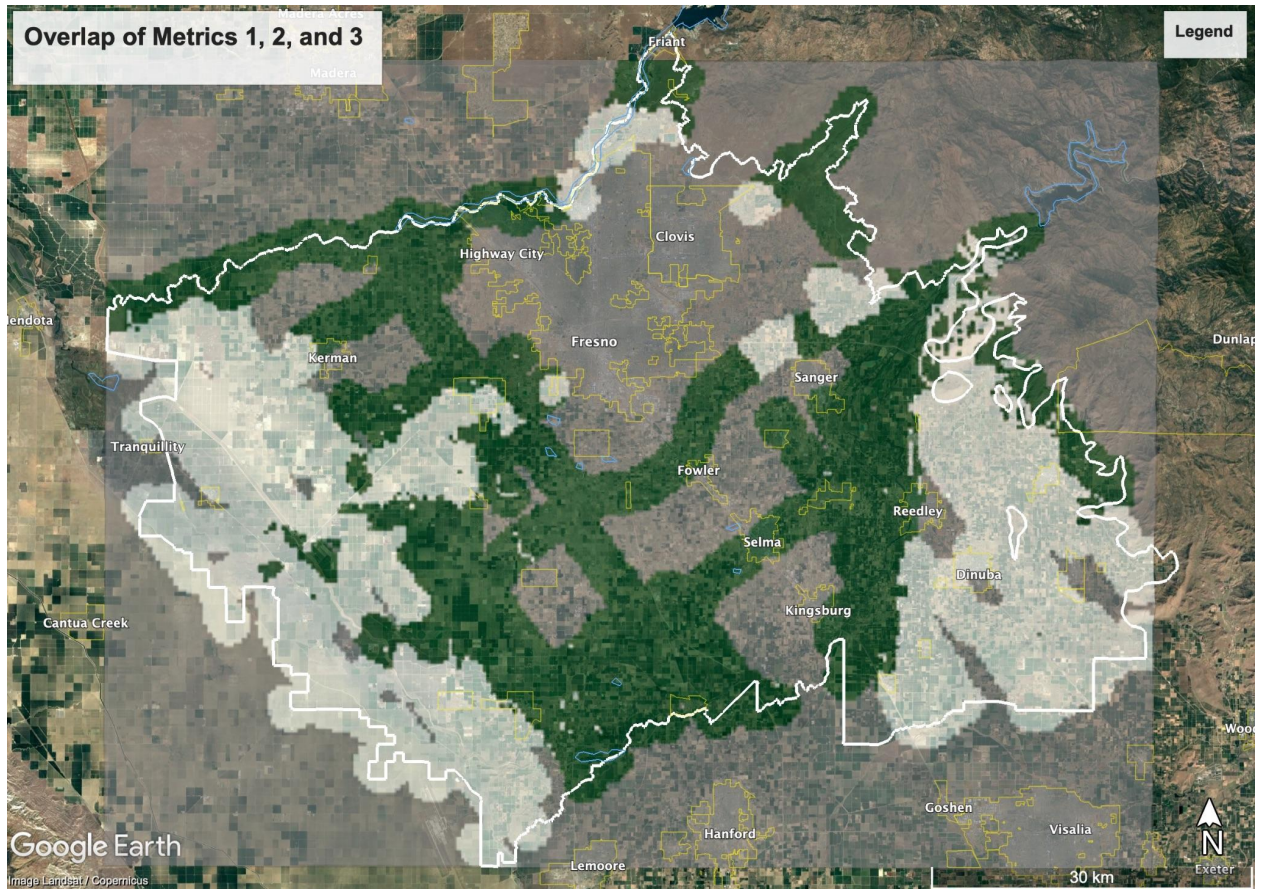


(10-1, Depth to no-flow unit in Kings Subbasin, generated by *fastpath*)

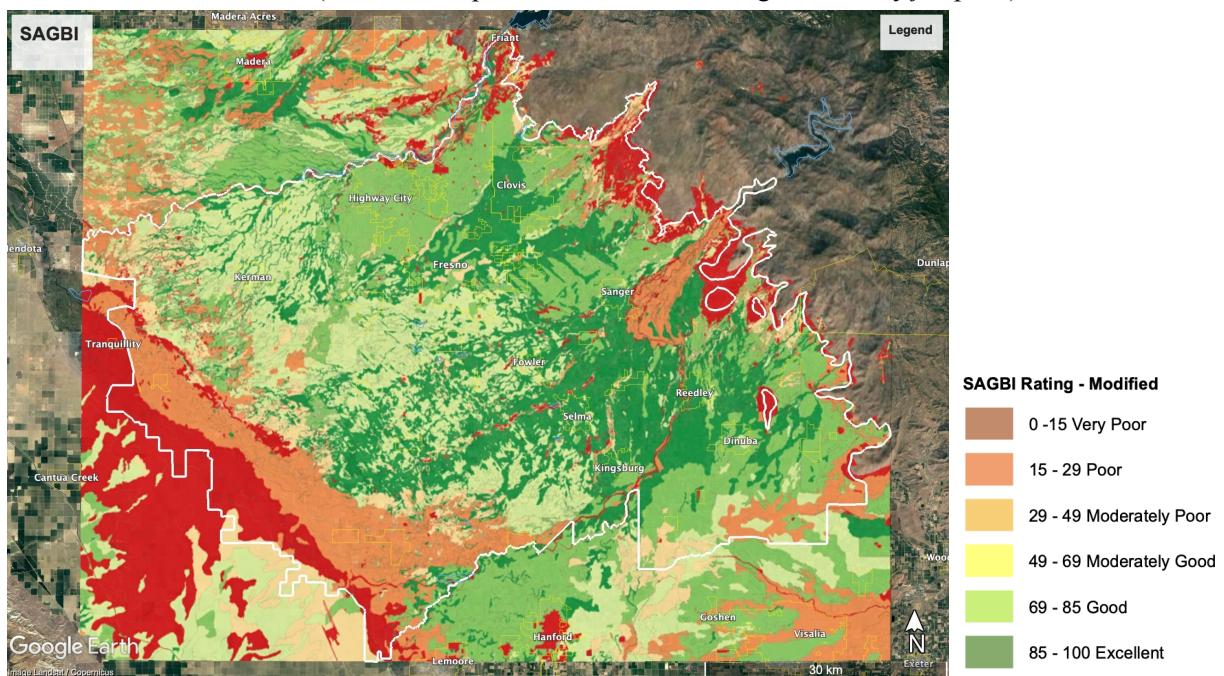
11. Recommendation in Selection of Recharge Sites

Overlay of Indexes

By combining the previous three metrics and SAGBI, we can narrow down potential recharge sites in the Kings Subbasin. As a reference, 11-1 is the overlapped area of metrics 1, 2, and 3 (fraction coarse-dominated > 90%, normalized path length < 2.01, depth to no-flow > 20m), and 11-2 is SAGBI (green is good, red is poor). It is important to note that each of these metrics is insufficient on its own. Fraction coarse-dominated is suited to get the general sense of whether there are a lot of coarse, permeable materials beneath a certain location, although it does not take into account the exact location or distribution of those materials. Normalized path length indicates how straight a path to the water table is, which helps us avoid locations with complicated paths to the water table, but this does not filter out locations best for recharge enough. Depth to no-flow is also a metric that helps us avoid locations not suited for recharge (places with the risk of ponding) but not necessarily pick the best place. SAGBI is a comprehensive factor with 5 different indexes but is limited to near-surface level (~2m). In fact, large parts of the eastern Kings Subbasin have "good" or "excellent" ratings for SAGBI (11-2) but not a good location according to the previous three metrics (11-1). This is presumably due to the shallow depth SAGBI takes into account.

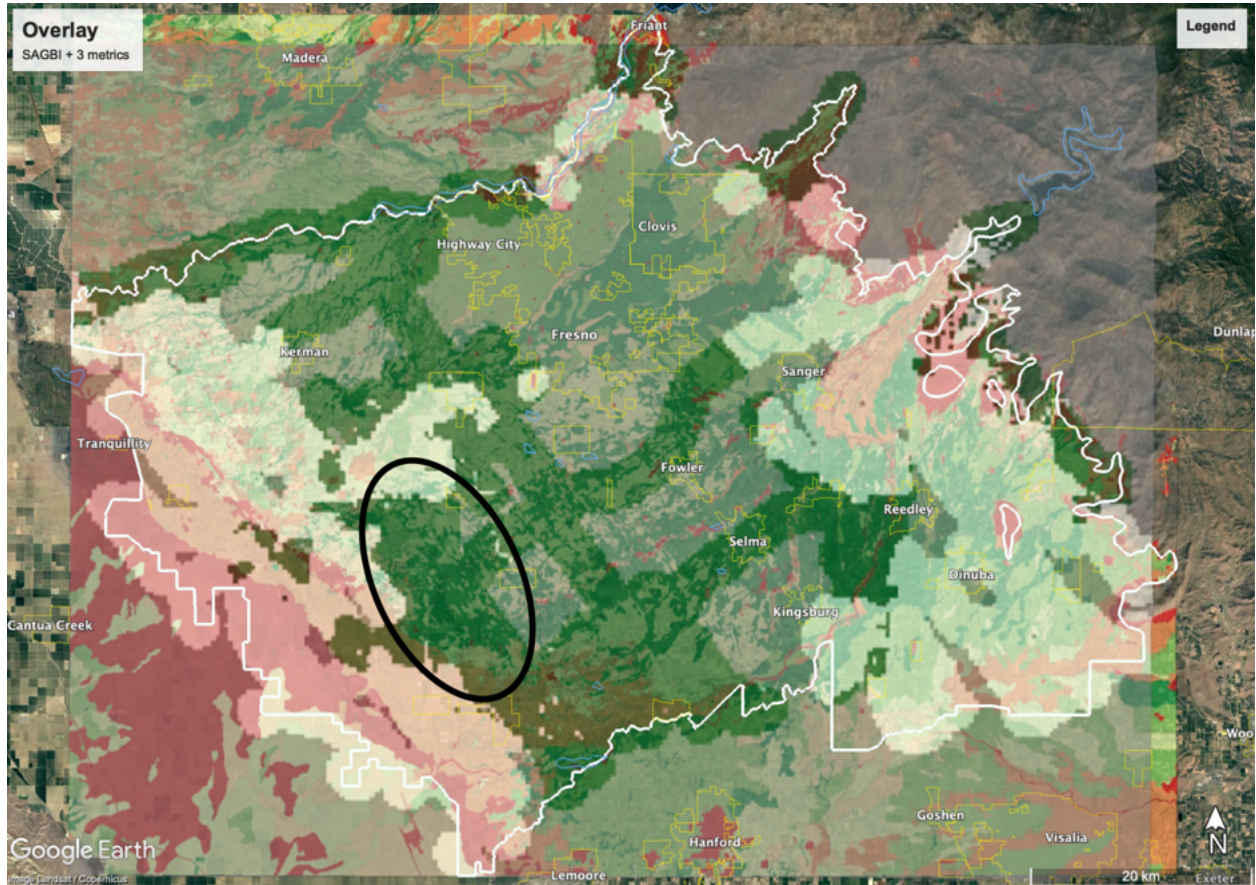


(11-1, Overlap of metrics 1, 2, and 3, generated by *fastpath*)



(11-2, SAGBI)

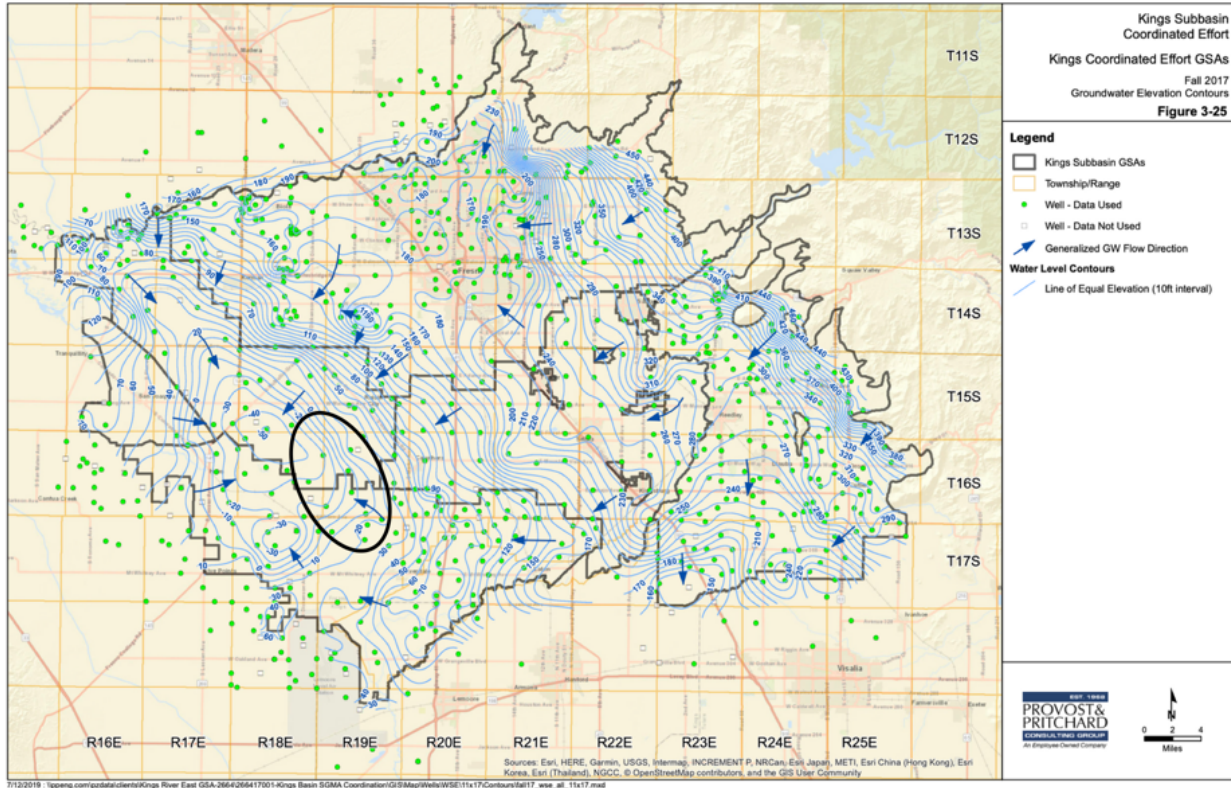
However, we can minimize the limitation of each metric by combining them, sorting out the "elite" locations that were noted positively by all the metrics. Below is the overlay of the two maps above (11-3). The greenest areas are the locations with positive ratings on both the three metrics and SAGBI. We can observe multiple greenest areas scattered over the central part of the subbasin.



(11-3, Overlay of three metrics and SAGBI, generated by *fastpath*)

Recommended Recharge Site and Groundwater Flow Direction

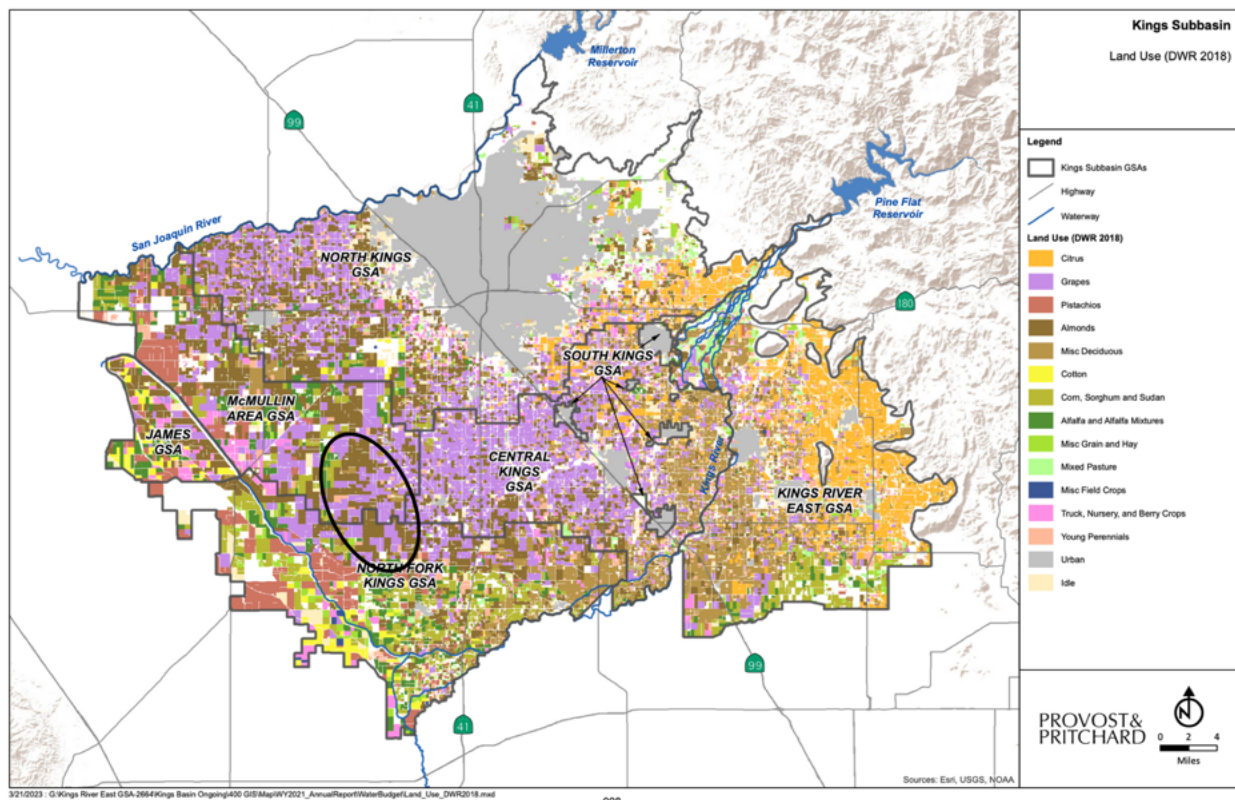
Groundwater recharge involves numerous factors and stakeholders, such as budget limits, the ownership of land, and regulations, and geological analysis cannot solely decide a perfect recharge site. However, based on our assessment, I suggest recharging the black-circled area in the western Kings Subbasin (11-3). 11-4 shows the groundwater flow direction in the subbasin. Groundwater generally flows eastward in the circled area, which implies that if we recharge a location in the circle, some portion of the supplied water flows eastward. Now recall Chapter 1, where we assessed the current situation and issue of the Kings Subbasin. The issue of overdraft and land subsidence was most serious on the western side of the subbasin (McMullin Area GSA and North Fork Kings GSA) (1-3, 1-4). Therefore, out of all the potential recharge sites, it makes the most sense to recharge a location where water can be conveyed to those problematic areas.



(11-4, North Kings GSP, 135, Groundwater flow direction)

Land use in the Recommended Recharge Site

Below is a map showing the agricultural land usage of Kings Subbasin (11-5). The circled area is mostly almond fields (brown) or vineyards (purple), reflecting the agriculture of Kings Subbasin. Vineyards are a strong candidate as a recharge site, as they have less soil nitrate in the profile and thus less nitrate contamination of recharged water (California Ag Network). In addition, as we discussed in Chapter 4, metal rods in vineyards cause noise to the AEM survey, and there are some areas lacking AEM data around the black circle due to this. However, these areas have high SAGBI ratings and are likely to have high metric evaluations as well, so there is a huge potential in recharging these unsurveyed areas. Therefore, I suggest a more local scale geologic survey (e.g., Towed EM survey) to acquire additional data in and around the black circle to fill in the gaps.



(11-5, North Kings GSA, 135, Land use in Kings Subbasin)

Previous Recharge Projects and Water Conveyance

As we discussed in Chapter 2, multiple groundwater recharge projects that have been taking place in Kings Subbasin. Below is the map of 15 dedicated basins that had been constructed or are in development in the span of January 2020 to November 2021 (11-6, Kings River Conservation Project). We can see that there is an existing reservoir for recharge in the recommended area (Terra Linda Recharge Project 2). Although we were not able to obtain accurate and up-to-date information about the water conveyance system in Kings Subbasin, the presence of a recharge project suggests that the water conveyance system has at least reached this recharge site, which means that it is feasible to extend the conveyance system to the recommended area without too much construction.



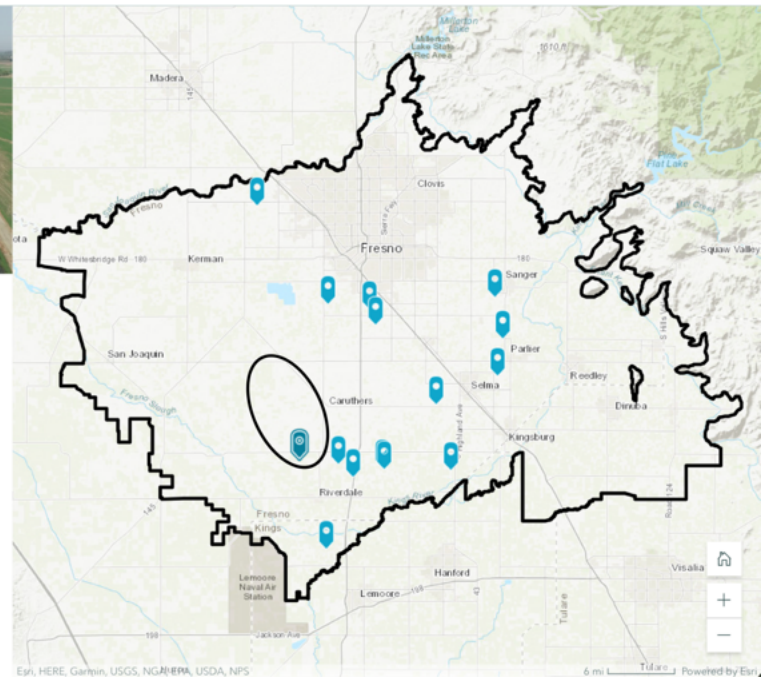
Terra Linda Recharge Project 2

Estimated Avg. Recharge Capacity: 400 Acre Feet/Year

Project Sponsor: Liberty Mill Race Company, a mutual water company

GSA: North Fork Kings GSA

Project Details: 20 acres. Landowner constructed project; may primarily be used as a storage reservoir.



(11-6, Kings River Conservation Project, Previous Recharge Projects)

Conclusion

Based on the four metrics (integrated fraction coarse-dominated, normalized path length, depth to no-flow, SAGBI), proximity to regions with overdraft and land subsidence, recharge-suited land use, and the feasibility of water conveyance, I recommend the circled area in 11-3 as the recharge site. As I mentioned before, groundwater recharge is a large-scale project, and its practicability depends on various other factors such as budget, land ownership, and regulations. In addition, although we have a general sense of the groundwater flow direction, we cannot precisely track where the water flows once it permeates into the subsurface. Needless to say, many more layers of additional research, planning, and negotiation are required to realize a recharge project. Yet, this assessment of recharge potential provides the initial step to sustainable agriculture and urban life in the Kings Subbasin through effective groundwater recharge.

Reference

Auken, Esben. Christiansen, Anders Vest. 2011. A global measure for depth of investigation. *GEOPHYSICS*. Accessed April 30, 2023.
<https://library.seg.org/doi/10.1190/geo2011-0393.1>

California Ag Network, *Vineyards Serve as Ideal Groundwater Recharging Sites*, Accessed June 3, 2023.
<https://californiaagnet.com/2021/02/09/vineyards-serve-as-ideal-groundwater-recharging-sites/>

California Department of Water Resources, *Airborne Electromagnetic (AEM) Surveys Data*, accessed May 15, 2023.

<https://data.cnra.ca.gov/dataset/aem>

California Department of Water Resources. *San Joaquin Valley Groundwater Basin Kings Subbasin*. California's Groundwater (Bulletin 118). Accessed April 15, 2023.

https://water.ca.gov/-/media/DWR-Website/Web-Pages/Programs/Groundwater-Management/Bulletin-118/Files/2003-Basin-Descriptions/5_022

Central Kings Groundwater Sustainability Agency. Groundwater Sustainability Plan. pp 046.

Department of Water Resources. *SGMA Portal*. Accessed June 5, 2023.

<https://sgma.water.ca.gov/portal/gsp/all>

Development and Resource Management Department, City of Fresno. *Fresno General Plan*. 3-86-3-70. Accessed April 16, 2023.

https://www.fresno.gov/darm/wp-content/uploads/sites/10/2022/12/upload_temp_Consolidated-GP-10-13-2022.pdf

Employment Development Department. *REPORT 400 C Monthly Labor Force Data for Counties February 2023 - Preliminary*. Accessed April 15, 2023.

Fresno County Economic Development Corporation. *Fresno County*. Accessed April 16, 2023.

<https://www.fresnoedc.com/fresno-county/>

James Groundwater Sustainability Agency. Groundwater Sustainability Plan. Accessed April 23, 2023.
<http://jamesgsa.org/wp-content/uploads/2020/04/2019-1212%20James%20GSP%20Adopted.pdf>

Kings River Conservation Project, *Kings Subbasin Builds for Drought Resilience at Record Pace*. November 12, 2021. Accessed April 20, 2023.

<https://storymaps.arcgis.com/stories/215f23039c0341e9b4d9bcd7fc125f80>

Kings Subbasin Groundwater Sustainability Agencies. *Groundwater Sustainability Annual Report Water Year 2022*. Accessed April 15, 2023.

https://northkingsgsa.org/wp-content/uploads/2023/04/5-022.08_Kings_WY_2022.pdf

Kings River East Groundwater Sustainability Agency. Groundwater Sustainability Plan. pp 65.

Kings Subbasin Groundwater Sustainability Agencies. *Kings Subbasin Coordination Agreement*. Accessed April 16, 2023.

<https://www.mcmullinarea.org/wp-content/uploads/2023/02/Kings-Coordination-Agreement-fully-execute-d-12-20-2019-revExB.pdf>

Knight, Rosemary. *Resistivity-to-Sediment-Type Transform*. Geophysics 190, Stanford University.

McMullin Area Groundwater Sustainability Agency. Groundwater Sustainability Plan. Accessed April 17, 2023.

<https://www.usbr.gov/watersmart/watermarketing/docs/applications/2018/McMullin%20Area%20Groundwater%20Sustainability%20Agency.pdf>

MyGeodata Cloud. Vineyards in California State. OpenStreetMap. Accessed May 2, 2023.

<https://mygeodata.cloud/data/download/osm/vineyards/united-states-of-america--california>

North Fork Kings Groundwater Sustainability Agency. Groundwater Sustainability Plan. pp. 2-13. Accessed April 23, 2023.

https://northforkkings.org/webpages/wp-content/uploads/2020/01/NFKGSA_GSP_Final_Adopted.pdf

North Kings Groundwater Sustainability Agency. Groundwater Sustainability Plan. Accessed April 17, 2023.

<https://northkingsgsa.org/groundwater-sustainability-plan/>

Quist, Rebecca. Advance Groundwater Sustainability Project Construction. North Kings Groundwater Sustainability Agency. June 29, 2022. Accessed April 20, 2023.

<https://northkingsgsa.org/kings-subbasin-awarded-7-6-million-grant-from-ca-department-of-water-resources-to-advance-groundwater-sustainability-project-construction/>

South Kings Groundwater Sustainability Agency. Groundwater Sustainability Plan.

Stanford, Doerr School of Sustainability. *fastpath*. Groundwater Recharge. Accessed May 20, 2023.

<https://fastpath-web.curvenote.dev/>

United States Department of Agriculture. *Fresno County, Census of Agriculture Fresno Country Profile (2017)*. Accessed April 16, 2023.

https://www.nass.usda.gov/Publications/AgCensus/2017/Online_Resources/County_Profiles/California/cp_06019.pdf